



Investigating the Impact of Simulation Fidelity on Automotive Decision-Making

Master's thesis in Computer Science and Engineering

**ANTON GOLE
HUNG LE**

MASTER'S THESIS 2025

Investigating the Impact of Simulation Fidelity on Automotive Decision-Making

ANTON GOLE
HUNG LE



UNIVERSITY OF
GOTHENBURG



CHALMERS
UNIVERSITY OF TECHNOLOGY

Department of Computer Science and Engineering
CHALMERS UNIVERSITY OF TECHNOLOGY
UNIVERSITY OF GOTHENBURG
Gothenburg, Sweden 2025

Investigating the Impact of Simulation Fidelity on Automotive Decision-Making
ANTON GOLE, HUNG LE

© ANTON GOLE, HUNG LE, 2025.

Supervisor: Felix Cherubini, Computer Science and Engineering
Supervisor: Sergei Borzov, Volvo Cars
Examiner: Ana Bove, Computer Science and Engineering

Master's Thesis 2025
Department of Computer Science and Engineering
Chalmers University of Technology and University of Gothenburg
SE-412 96 Gothenburg
Telephone +46 31 772 1000

Cover: Example image taken from inside our simulation in the game engine Unreal Engine 5.

Typeset in L^AT_EX
Gothenburg, Sweden 2025

Investigating the Impact of Simulation Fidelity on Automotive Decision-Making

ANTON GOLE

HUNG LE

Department of Computer Science and Engineering

Chalmers University of Technology and University of Gothenburg

Abstract

This thesis examines how *visual* rendering choices of a driving simulator changes how a camera-based Automated Emergency Braking (AEB) behaves. Scenario logic, perception, decision, and actuation are held fixed; only the visual rendering varies. One lower-detail baseline is compared with forty higher-detail settings that switch shadows on/off, change the sky, add roadside elements (trees, grass, rocks), and vary the sun's height and direction across sixteen scenarios. We record AEB activation time, activation distance, Time-to-Collision at activation, and whether activation occurs.

As a sanity check, we first confirm that results are closely matched when advanced visual effects are turned off in two independent implementations of the simulator (typical differences about 23%). Within the higher-detail variants, effects are context-dependent rather than uniform. Low sun elevation (10° above the horizon) consistently reduced safety margins: on average AEB triggers roughly 1 m closer and about 0.05 s later. Higher visual detail also exposed hidden failures: in 5 of 16 scenarios, at least one higher-detail run did not activate AEB while the baseline did (15/640 runs; 2.3% overall; per-scenario failure rates roughly 221%).

Overall, visual settings—especially sun angle—can change AEB timing and occasionally prevent activation. We note limitations (camera-only system and sparse failures), and recommend reporting visual settings and testing across varied lighting and scene complexity when using simulation for ADAS evaluation.

Keywords: simulation fidelity; visual rendering; Automated Emergency Braking (AEB); Advanced Driver-Assistance Systems (ADAS); closed-loop simulation; high-fidelity configurations.

Acknowledgements

This master's thesis was carried out at Volvo Cars in Göteborg. We would like to express our sincere gratitude to our supervisors, Felix Cherubini (Department of Computer Science and Engineering) and Sergei Borzov (Volvo Cars), for their guidance, constructive feedback, and support throughout the project. We are also grateful to our examiner, Ana Bove (Department of Computer Science and Engineering), for her insightful comments and careful review.

We thank Volvo Cars for hosting the work and for providing the resources, data, and stimulating environment that made this study possible. The discussions with colleagues at Volvo Cars greatly helped refine our experimental design and interpretation of results related to simulation fidelity.

Anton Gole, Hung Le, Gothenburg, 2025-10-20

List of Acronyms

AAE	Average Attribute Error
ADAS	Advanced Driver-Assistance Systems
ADS	Automated Driving Systems
AEB	Automated Emergency Braking
API	Application Programming Interface
ASAM	Association for Standardisation of Automation and Measuring Systems
ATE	Average Translation Error
AOE	Average Orientation Error
ASE	Average Scale Error
AVE	Average Velocity Error
CCC	Concordance Correlation Coefficient
CI	Confidence Interval
CI/CD	Continuous Integration / Continuous Delivery
C2C	Car-to-Car
EPV	Events per Variable
DLOD	Deep Learning Object Detection
FCOS3D	Fully Convolutional One-Stage 3D Detector
FIFO	First In, First Out
GI	Global Illumination
GPU	Graphics Processing Unit
HDF5	Hierarchical Data Format version 5
HDR	High Dynamic Range
ICC	Intraclass Correlation Coefficient
ID	Identifier

ISO	International Organization for Standardization
JSON	JavaScript Object Notation
LBFGS	Limited-memory Broyden-Fletcher-Goldfarb-Shanno
LoA	Limits of Agreement
LiDAR	Light Detection and Ranging
LOD	Level of Detail
mAP	mean Average Precision
NDS	nuScenes Detection Score
NCAP	New Car Assessment Programme
OR	Odds Ratio
OSI	Open Simulation Interface
PCG	Procedural Content Generation
RMSE	Root Mean Square Error
SDF	Signed Distance Field
SOTIF	Safety of the Intended Functionality
TCP	Transmission Control Protocol
TTC	Time-To-Collision
UDP	User Datagram Protocol
UE5	Unreal Engine 5
URP	Universal Render Pipeline
VRU	Vulnerable Road User
XML	Extensible Markup Language
ZMQ	ZeroMQ

Nomenclature

Variables

Δt	Fixed simulation step size (25 ms; logged as 2.5×10^7 ns)
Δy_{is}	Within-scenario change from baseline in outcome y for run i of scenario s
$\Delta\mathcal{D}$	Change in decision output between fidelity conditions
\dot{v}_{ego}	Time-derivative of ego-vehicle speed (m s^{-2})
\dot{y}	Lateral velocity (m s^{-1})
\hat{p}_s	Estimated failure rate for scenario s
$\mathbb{1}_{\text{no-AEB}}$	Indicator: 1 if no AEB activation observed, else 0
\mathbf{p}_{ego}	Position vector of the ego vehicle (m)
\mathbf{p}_{lead}	Position vector of the lead (front) vehicle (m)
\mathbf{v}_{ego}	Velocity vector of the ego vehicle (m s^{-1})
\mathbf{v}_{lead}	Velocity vector of the lead vehicle (m s^{-1})
\mathcal{A}	Actuator (vehicle-control) model in closed-loop diagram
\mathcal{D}	Decision-making module in closed-loop diagram
\mathcal{P}	Perception module in closed-loop diagram
$\mathcal{S}_{\text{logic}}$	Scenario-execution layer (<code>esmini</code>) in closed-loop diagram
TTC	Time-to-Collision computed from relative range and speed (s)
TTC _{AEB}	Time-to-Collision at AEB activation (s)
C_s	Failure count in scenario s
d_{AEB}	Longitudinal distance to lead at AEB activation (m)
R	Rendering module that varies between fidelity conditions
s	Reference-line arc-length coordinate in OpenDRIVE s - t frame (m)

t	Lateral offset from the reference line in OpenDRIVE s - t frame (m)
t_{AEB}	AEB activation time (ms; logged in ns)
v	Vehicle speed (m s^{-1})
x	Cartesian longitudinal position (m)
y	Cartesian lateral position (m)
$y_s^{(\text{base})}$	Scenario- s baseline value (UE5 fidelity-off) for outcome y
z	Vertical position / altitude (m)
$z_{0.975}$	Standard-normal 97.5% quantile used in Wilson interval

Special terms

Actor	Any entity in OpenSCENARIO able to perform actions (vehicles, pedestrians, etc.)
Closed-loop	Simulation where perception outputs steer the virtual vehicle each step
Dynamic actor	An actor with a scripted trajectory and behaviour
Ego vehicle	The vehicle of interest during simulation tests
esmini	Light-weight OpenSCENARIO/OpenDRIVE player used as scenario engine
GameInstance	Unreal Engine's top-level manager for a running application instance.
Lumen	Unreal Engine's dynamic global-illumination system
Nanite	Unreal Engine's virtualised geometry system
Path Tracer	Unreal Engine's offline unbiased renderer
PCG pipeline	Procedural-Content-Generation workflow for virtual environments
Perception stack	Sequence of detection, tracking and classification modules
Scenario	Complete description of roads, traffic and triggers used as an experiment
Time-to-Collision	Time needed to close the gap under current relative speed

Contents

List of Acronyms	ix
Nomenclature	xi
List of Figures	xvii
List of Tables	xix
1 Introduction	1
1.1 Background	1
1.2 Testing & Simulation	1
1.3 Problem Statement	2
1.4 Objectives	2
1.5 Scope and Limitations	3
2 Theory	5
2.1 Simulation Fidelity	5
2.2 ASAM OpenX Standards for Scenario-Based Simulation	5
2.2.1 OpenDRIVE — Road-Network Geometry	6
2.2.2 OpenSCENARIO XML — Dynamic Actors and Logic	6
2.2.3 Open Simulation Interface (OSI)	7
2.3 esmini — A Lightweight OpenSCENARIO Player	7
2.4 Closed-Loop Testing Architecture	8
2.4.1 Definition of "Closed-Loop Simulation"	9
2.5 Performance-Evaluation Metrics	9
2.5.1 AEB Activation Time t_{AEB}	9
2.5.2 Distance to Lead Object at AEB Activation d_{AEB} (longitudinal) .	10
2.5.3 Time-to-Collision at AEB Activation TTC_{AEB} (longitudinal) .	10
2.5.4 Alignment with Safety Standards	10
2.6 Core Perception Module: Zenseact DLOD	11
2.6.1 Why FCOS3D?	11
2.6.2 Key Design Choices	11
2.6.3 Performance	12
2.7 Game-Engine Rendering Pipelines	12
2.7.1 Unity URP (Low-Fidelity Baseline)	12
2.7.2 Unreal Engine 5 + Lumen/Path Tracing (High Fidelity) . . .	12

2.7.2.1	Why UE5 for the fidelity sweeps	12
2.7.2.2	Nanite Virtualized Geometry	12
2.7.2.3	Lumen Dynamic Global Illumination	13
2.7.2.4	Theoretical Expectations	13
3 Methods		15
3.1	Architecture overview	15
3.1.1	Implemented Software Components	16
3.2	Inter-Process Communication	16
3.2.1	Message layout	16
3.3	UE5 endpoint	17
3.3.1	Init	18
3.3.2	Pre-tick — receive updated poses	18
3.3.3	Post-tick — broadcast data to other processes	19
3.4	<code>esmini</code> endpoint	19
3.5	Timing and Determinism	20
3.6	Scene construction and coordinate systems	20
3.6.1	Road-mesh builder	21
3.6.2	Procedural generation	21
3.6.3	Camera setup	22
3.7	Synchronous image loop	22
3.8	Game-Engine Alignment	23
3.8.0.0.1	Motivation for the cross-engine baseline check.	24
3.9	Experimental Scenarios	24
3.9.1	NCAP-derived Safety Scenarios	26
3.10	Data Gathering and Processing	27
3.10.1	Signals and derived metrics.	27
3.10.2	Scenario Identifiers	28
3.10.3	Low vs. High Fidelity Mapping	28
3.10.4	Cross-Simulator Baselines	28
3.11	Statistical Analysis	28
3.11.1	Decompose the Research Questions	28
3.11.2	Analyzed metrics	28
3.11.3	Baseline alignment across scenarios (Unity vs UE5, fidelity-off)	29
3.11.3.0.1	Rationale for approach.	29
3.11.3.0.2	Setup and pairing.	29
3.11.3.0.3	Reporting (simple matched-pairs summaries).	29
3.11.3.0.4	Visualization.	29
3.11.3.0.5	Assumptions.	30
3.11.4	Fidelity effects on continuous outcomes	30
3.11.4.0.1	Design and predictors.	30
3.11.4.0.2	Estimation and uncertainty.	30
3.11.4.0.3	Rationale.	31
3.11.4.0.4	Interpretation.	31
3.11.5	Failure exposure	31
3.11.6	Logistic regression for failure predictors	31

3.11.6.0.1	Outcome and scope.	31
3.11.6.0.2	Rationale.	32
3.11.6.0.3	Predictors and coding.	32
3.11.6.0.4	Estimation.	32
3.11.6.0.5	Cluster bootstrap for uncertainty.	32
3.11.6.0.6	Reporting and interpretation.	33
3.11.7	Robustness and exclusions	33
4	Results	35
4.1	Data Overview	35
4.2	Baseline Alignment: Cross-Simulator Validation	35
4.2.1	Fidelity effects on continuous outcomes	38
4.3	Failure Mode Exposure	39
4.3.1	Logistic regression of failure on fidelity factors	40
5	Discussion	41
5.1	What the baseline validation establishes	41
5.2	How fidelity changes AEB activation margins	41
5.3	Higher fidelity exposes hidden non-activations	42
5.4	Interpreting the failure model	42
5.5	Practical implications for simulation-based ADAS testing	42
5.6	Methodological reflections	43
5.7	Threats to validity and limitations	43
5.8	Future work	44
Bibliography		45
A Appendix 1		I

Contents

List of Figures

2.1	Reference-line-based s - t coordinate system with origin at the beginning of the road.	6
2.2	Screenshot of a 3D scene rendered by <code>esmini</code> . The minimal rendering style highlights lane-level and object-ground truth structure, but lacks dynamic lighting and high-fidelity textures. This rendering is typically used for debugging or visualization, while image-based sensor testing requires an external engine such as Unity or Unreal.	8
2.3	Demonstration of Lumen global illumination in UE5.	13
3.1	Per-step synchronization between <code>esmini</code> , UE5, and the vision stack. <code>esmini</code> sends the step state (Tick), UE5 renders and conditionally ships the image to the vision stack, then acknowledges the same step (Tock).	23
3.2	Effect of enabling each of the three fidelity factors. Shadows use a zenith sun (90° elevation) in all images.	25
3.3	Effect of sun elevation angle on lighting and shadows, with sun fixed in the west. From left to right: 90° (zenith), 45° , and 10° above the horizon. Lower sun angles produce longer, softer shadows and warmer lighting effects.	25
4.1	Direct comparison (scatter): Unity values (x) vs. UE5 (fidelity-off) values (y) with the identity line $y = x$. Points close to the identity line indicate strong baseline comparability.	37
4.2	Difference-vs-average plots: per scenario, the paired difference Δ (UE5 off – Unity) is shown against the scenario average. The solid line is the mean difference $\bar{\Delta}$; dashed lines show $\bar{\Delta} \pm t_{0.975,15} \cdot \text{SD}(\Delta)$ with $t_{0.975,15} \approx 2.13$, illustrating the typical spread.	38

List of Figures

List of Tables

3.1	FIFOs used for synchronization.	16
3.2	Visual-fidelity factors explored in UE5	24
3.3	Sun-light directions tested when <i>shadows</i> = <i>On</i>	25
3.4	NCAP scenarios and initial conditions	27
4.1	Baseline alignment (Unity vs UE5, fidelity=off): matched-pairs summaries. $\Delta = \text{UE5}_{\text{off}} - \text{Unity}$	35
4.2	Per-scenario <i>symmetric</i> absolute percentage differences for baseline alignment. Percentage difference is $100 \times \frac{2 m_s^{(\text{UE5_off})} - m_s^{(\text{Unity})} }{ m_s^{(\text{UE5_off})} + m_s^{(\text{Unity})} }$	36
4.3	Ridge linear model for Δd_{AEB} (metres); scenario-cluster bootstrap 95% CI.	39
4.4	Ridge linear model for $\Delta \text{TTC}_{\text{AEB}}$ (seconds); scenario-cluster bootstrap 95% CI.	39
4.5	Scenarios where higher fidelity exposed AEB failures (EyeCar activated successfully).	39
4.6	Ridge-penalized logistic regression predicting AEB non-activation. Odds ratios (OR) with 95% scenario-cluster bootstrap CIs; baseline is Shadow=off, PCG=off, Sky=white, Elevation=90°.	40
A.1	AEB metrics for scenario: Car to Car front turn across path (ccf-tap_speed_20_45)	II
A.2	AEB metrics for scenario: Car to Car front turn across path (ccf-tap_speed_20_60)	III
A.3	AEB metrics for scenario: Car to Car Rear braking (ccrb_decel_6) .	IV
A.4	AEB metrics for scenario: Car to Car Rear braking (ccrb_decel_2) .	V
A.5	AEB metrics for scenario: Car to Car Rear moving (ccrm_speed_50) .	VI
A.6	AEB metrics for scenario: Car to Car Rear moving (ccrm_speed_80) .	VII
A.7	AEB metrics for scenario: Car to Car Rear stationary (ccrs_speed_50)	VIII
A.8	AEB metrics for scenario: Car to Car Rear stationary (ccrs_speed_80)	IX
A.9	AEB metrics for scenario: Car to Pedestrian Farside Adult (cpfa_speed_50)	X
A.10	AEB metrics for scenario: Car to Pedestrian Farside Adult (cpfa_speed_60)	XI
A.11	AEB metrics for scenario: Car to Pedestrian Longitudinal Adult (cpla_speed_50)	XII
A.12	AEB metrics for scenario: Car to Pedestrian Longitudinal Adult (cpla_speed_80)	XIII
A.13	AEB metrics for scenario: Car to Pedestrian Nearside Adult (cpna_speed_50)	XIV

List of Tables

A.14 AEB metrics for scenario: Car to Pedestrian Nearside Adult (cpna_speed_60)	XV
A.15 AEB metrics for scenario: Car to Pedestrian Nearside Child Obstructed (cpnco_speed_50)	XVI
A.16 AEB metrics for scenario: Car to Pedestrian Nearside Child Obstructed (cpnco_speed_60)	XVII

1

Introduction

Autonomous driving technologies, in their current state, are no longer experimental. Partial automation functions such as lane centering and Automated Emergency Braking (AEB) are now delivered in millions of production cars. As the scope of these so-called Advanced Driver-Assistance Systems (ADAS) expands, every software update must be evaluated for safety-relevant performance across a wide variety of traffic, weather, and lighting conditions. Exhaustive road testing is economically unfeasible, so industry practice has shifted toward large-scale, *closed-loop simulation* (the perception-decision outputs are fed back to move the virtual car; see Sec. 2.4.1).

1.1 Background

Road transport remains an important but dangerous activity of modern society. According to the World Health Organization, in 2021 more than 1.19 million people were killed in traffic accidents. In 2019, road injuries were the leading cause of death for children and young people aged 5 to 29, and the 12th leading cause of death across all age groups, according to the same source [1]. Advanced Driver-Assistance Systems (ADAS) and their higher-level successors, Automated Driving Systems (ADS), have been introduced in many vehicles for this reason. These systems combine camera, radar, and Light Detection and Ranging (LiDAR) sensing with onboard intelligence to keep the vehicle in its lane, monitor blind spots, and even perform emergency manoeuvres [2].

Since the first production anti-lock braking system was introduced in 1978, vehicle automation has steadily increased in sophistication [3]. Modern vehicles offer Level 2 (partial automation) and even Level 3 (conditional automation) capabilities [2]. In parallel, the European Commission now requires the inclusion of features such as Collision Avoidance, Intelligent Speed Adaptation and Automated Emergency Braking in new vehicles [4]. Ensuring the safety of these increasingly complex, learning-based systems can be a challenge. As a result, the verification process has become a major bottleneck.

1.2 Testing & Simulation

Automotive testing traditionally occurs in both real-world conditions and controlled simulations. While real-world testing provides direct validation, it is expensive, time-

consuming, and limited in scope. Simulation-based testing in virtual environments offers a scalable alternative, allowing manufacturers to evaluate decision-making systems under diverse scenarios and environmental conditions. Within such virtual worlds, *simulation fidelity*—the level of realism in geometry, lighting, shadows, materials, and environmental detail—becomes a critical variable. Depending on the software stack, graphic settings, and scene-generation techniques, fidelity can range from minimalist shading to high-fidelity real-time global illumination. Whether pushing to the upper end of the fidelity spectrum can affect an ADAS controller’s continuous behaviour remains an open question. In this thesis we therefore compare a low-fidelity rendering pipeline (baseline) with a higher-fidelity pipeline that enables shadows, richer illumination, and procedural scene content; all other closed-loop components are held constant.

1.3 Problem Statement

Research to date has focused on frame-wise perception accuracy, yet little is known about how visual fidelity influences the controller’s decision-making. Does a photo-realistic scene have no impact, or does it influence the automated system’s decision-making, in particular the timing and conditions of Automated Emergency Braking, and to what extent? This thesis addresses the question by using both high- and low-fidelity scenes—under varying lighting, shadow qualities, and environmental richness—to measure their impact on an industry-grade decision-maker. We also investigate whether certain real-world faults (e.g., misdetections caused by glare) can be recreated only at higher fidelity, which would provide evidence that advanced rendering may be essential.

Below are the two questions this thesis aims to answer:

1. Does increased simulation fidelity lead to detectable changes in ADAS behaviour?
2. Can advanced rendering and richer scene complexity reproduce or expose failure modes that remain hidden in low-fidelity simulation?

1.4 Objectives

The work is organized around five objectives:

- **Adopt a More Capable Rendering Engine:**

We migrate from the existing Unity baseline [5] to Unreal Engine 5 (UE5) for the *fidelity sweeps*. Two practical needs motivated this choice. First, UE5’s Nanite geometry (see section 2.7.2.2) plus the built-in Procedural Content Generation (PCG) framework let us populate dense roadside clutter (trees, grass, rocks) at scale. Second, UE5’s Lumen provides *dynamic, physically based* global illumination and soft shadows out of the box, which made our sun-angle manipulations straightforward. To keep scenario logic, geometry, and materials consistent across engines, we export identical scenes to both

renderers and then *verify* that Unity and UE5 with all fidelity features disabled are closely aligned (Sec. 3.8, §3.11). All subsequent factor analyses are within UE5 relative to its fidelity-off baseline.

- **Define and Implement Metrics Beyond Pass/Fail:**
Alongside pass/fail, extract continuous AEB metrics (activation time, Time-to-Collision (TTC), distance at activation) to capture subtle behavioural shifts, and compare them across fidelity levels using the statistical approach outlined in §3.11.
- **Automatic Generation of Scenes from Road Descriptions:**
Create a tool for automatically generating scenes from road descriptions by incorporating high modularity, and leveraging UE5 capabilities for procedural generation.
- **Run Simulations in Varying Fidelity Levels and Potential Corner Cases:**
Run simulated scenarios in low-fidelity Unity and high-fidelity UE5. Additionally, incorporate or modify scenarios to approach failure conditions and replicate real-world 'challenging' situations, such as harsh lighting and cluttered environments.
- **Analyze differences with agreement metrics and cluster-aware models:**
Assess cross-simulator baseline alignment using matched pairs, reporting the mean paired difference with a 95% t -interval, RMSE, the maximum absolute difference, and symmetric percentage differences; we also visualize agreement with identity-line scatter plots and difference-vs-average plots; model within-scenario shifts in continuous outcomes via ridge linear regression with scenario-level cluster bootstrap; summarize per-scenario failure rates with Wilson score intervals; and relate fidelity factors to non-activation via ridge-penalized logistic regression with class_weight balancing and scenario-level cluster-bootstrap confidence intervals.

1.5 Scope and Limitations

This study focuses on *image-based* (camera) tests; no radar or LiDAR sensing is evaluated. Thus, certain aspects of real-world simulation are excluded:

- **No Audio-based Perception:**
No sound inputs (sirens, honking, road noise) are included. The study centers on visual-based sensor evaluations.
- **Rendering Constraints in UE5:**
While increasing scene fidelity, certain camera imperfections (auto-exposure, high dynamic range (HDR)) or complex lighting effects such as lens flares are not simulated.

Because we vary only camera-based visual fidelity with a single perception stack and

1. Introduction

forward-camera setup, our results support claims about *sensitivity* (how behaviour can change with visual conditions), not general guarantees across stacks, sensors, or vehicle dynamics. Conclusions should therefore be read as evidence that fidelity can both reveal and mitigate issues in perception-driven AEB, rather than as absolute performance judgments.

2

Theory

This chapter explains the pieces of our closed loop and how they connect. *Open-DRIVE* defines the road network; *OpenSCENARIO* defines actors and their behaviours. *esmini* (a lightweight OpenSCENARIO/OpenDRIVE player; see §3.4) advances the scenario in fixed steps and exposes the world state (poses, IDs, timestamps). The renderer (Unity or UE5) turns that state into camera images for the perception module, whose control outputs are applied by *esmini* on the next step. In all experiments, only the renderer varies; the rest of the perception–planning–control chain is fixed. For the implementation details, see Chapter 3, especially the architecture overview (§3.1).

2.1 Simulation Fidelity

Liu, Macchiarella and Vincenzi describe simulation fidelity as "the degree to which a simulation reproduces the state and behaviour of a real-world system in a measurable or perceivable manner" [6]. They distinguish several overlapping dimensions—physical, visual-audio, equipment, motion and psychological-cognitive.

For the purposes of this thesis, the term *simulation fidelity* refers solely to the *visual-audio* dimension: geometric detail, materials, lighting, shadows, and atmospheric effects that feed camera pipelines. All other dimensions (vehicle dynamics, equipment interfaces, motion cueing and audio ambience) are omitted so that any behavioural differences can be attributed to changes in visual realism alone.

2.2 ASAM OpenX Standards for Scenario-Based Simulation

Robust closed-loop testing of automated-driving functions depends on *interoperable* scene, map, and interface standards. The automotive industry has converged on the **ASAM** (Association for Standardisation of Automation and Measuring Systems) OpenX family [7], [8], [9], which allows different scenario players, traffic generators, sensor models, and control stacks to share a common digital ground-truth (the state of the virtual world). The three standards most relevant to this thesis are summarised below.

2.2.1 OpenDRIVE — Road-Network Geometry

ASAM OpenDRIVE describes the static road network—lane topology, elevation, superelevation, surface markings, signals, and other roadside objects—in a single `.xodr` (or compressed `.xodrz`) file [8]. Every element is parameterised along a one-dimensional reference line s with a lateral offset t . This curvilinear s - t frame allows accurate reconstruction in any render or physics engine, and forms the basis of the road-aligned coordinate system used in most scenario definitions.

As shown in Figure 2.1, the s - t system consists of two coordinate axes: the s -axis runs along the road’s reference line, while the t -axis points leftward orthogonal to it. This allows vehicle positions and lane elements to be defined in a road-relative frame, simplifying map-based localization and planning.

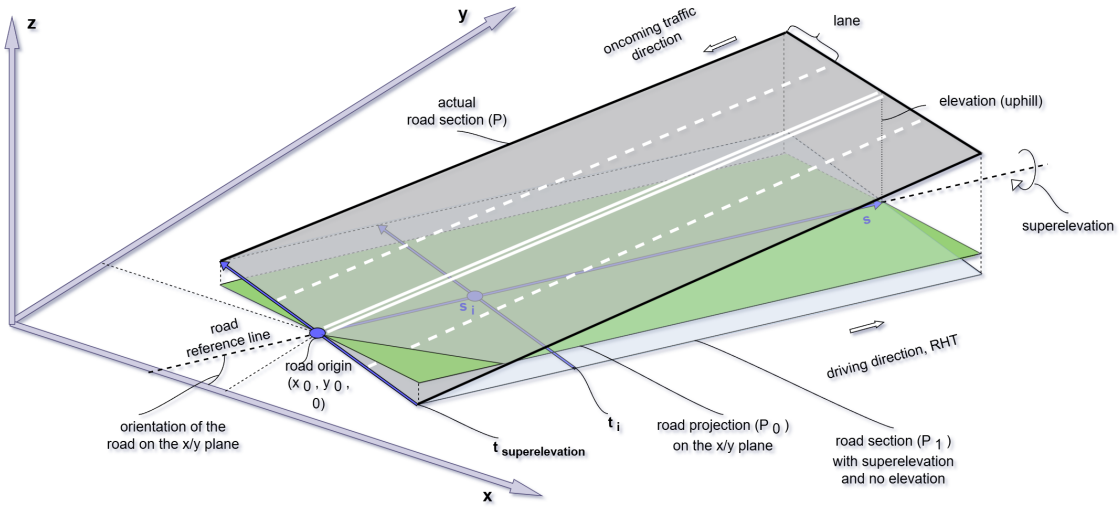


Figure 2.1: Reference-line-based s - t coordinate system with origin at the beginning of the road.

2.2.2 OpenSCENARIO XML — Dynamic Actors and Logic

Where OpenDRIVE is static, ASAM OpenSCENARIO Extensible Markup Language (XML) (`.xosc`) captures dynamic content—ego vehicle (the simulated car whose perception-planning stack is under test) and background entities, manoeuvres, trigger conditions, environmental parameters, and success criteria [7]. The language separates *what* happens (Actions inside Events) from *when and where* it happens (Start- and StopTriggers).

The behavioural model is hierarchical:

Story → Act → ManoeuvreGroup → Manoeuvre → Event → Action

This explicit layering enables both sequential and parallel execution. For instance, a merging *ManoeuvreGroup* may contain two vehicles whose lane-change Actions are synchronised by a Condition that waits for a safe gap. The schema maps cleanly onto deterministic simulation back-ends such as `esmini`.

2.2.3 Open Simulation Interface (OSI)

The Open Simulation Interface standardises run-time data exchange between simulation components via protocol-buffer messages [9]. OSI defines top-level messages for

- **GroundTruth**: ground-truth object list in a global frame.
- **SensorView** and **SensorData**: geometry clipped to a sensor field of view.
- **FeatureData**: mid-level perception features such as lane boundaries and object cues.
- **TrafficCommand/TrafficUpdate**: bidirectional control of traffic participants.
- **EgoControl**: actuation commands along the longitudinal (forward/reverse) and lateral (side-to-side) axes.

The message set allows both *modular* (component-in-the-loop) and *closed-loop* (software- or hardware-in-the-loop) evaluation by streaming sensor-level views into the stack and receiving actuation feedback.

2.3 esmini — A Lightweight OpenSCENARIO Player

`esmini` [10] is a minimalist yet capable scenario engine for OpenSCENARIO XML and OpenDRIVE. It can be used as a desktop viewer, a command-line batch runner, or a shared library embedded in custom pipelines.

At runtime, `esmini`

- parses OpenDRIVE road networks into an internal map representation.
- interprets OpenSCENARIO storyboards with deterministic fixed-step scheduling.
- exposes C/C++, Python, and C# application programming interfaces (APIs) for external controllers and observers.
- publishes OSI message streams (GroundTruth, SensorView, FeatureData) over User Datagram Protocol (UDP) or shared memory.

Entities such as the ego vehicle may therefore be driven by either script-defined Actions or an external closed-loop stack. Rendering is intentionally decoupled: `esmini` supplies ground-truth to Unity, Unreal, or custom renderers, keeping image generation outside the deterministic core. This architecture makes `esmini` a reproducible testbed for ADAS and ADS evaluation across a wide range of visual conditions.

`esmini`'s minimalistic renderer (Figure 2.2) does not include detailed lighting or texture effects, making it insufficient for realistic image-based sensor simulation. In practice, it is often embedded in larger simulation frameworks where high-fidelity

visuals are rendered by an external engine. This separation allows `esmini` to maintain deterministic behaviour and reproducibility while enabling advanced perception testing via more capable visual pipelines.

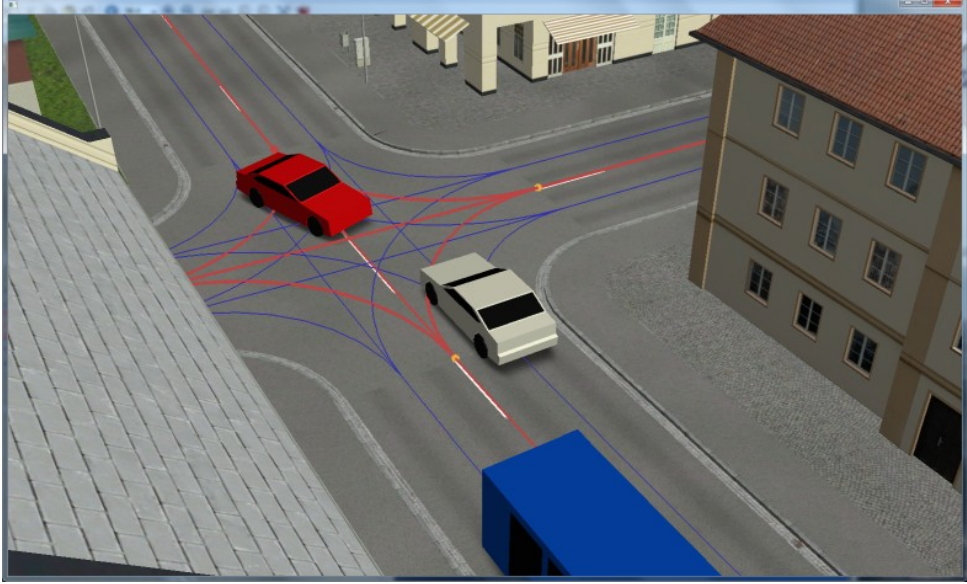


Figure 2.2: Screenshot of a 3D scene rendered by `esmini`. The minimal rendering style highlights lane-level and object-ground truth structure, but lacks dynamic lighting and high-fidelity textures. This rendering is typically used for debugging or visualization, while image-based sensor testing requires an external engine such as Unity or Unreal.

2.4 Closed-Loop Testing Architecture

From a theory perspective, the sensor-simulation loop can be modelled as the composition

$$\underbrace{\mathcal{S}_{\text{logic}}}_{\text{esmini}} \rightarrow \underbrace{R}_{\text{render pipeline}} \rightarrow \underbrace{\mathcal{P}}_{\text{perception}} \rightarrow \underbrace{\mathcal{D}}_{\text{decision-maker}} \rightarrow \underbrace{\mathcal{A}}_{\text{actuator model}}$$

Here, $\mathcal{S}_{\text{logic}}$ refers to the scenario execution layer implemented in `esmini`. It ensures logical consistency while being independent of rendering realism. Only the rendering module R varies between experimental conditions, enabling the isolation of visual fidelity as an independent variable.

All other blocks remain invariant, ensuring that any behavioural difference $\Delta\mathcal{D}$ originates in render-side fidelity variations [11]. This closed-loop structure reflects how fidelity influences the full decision-making chain in an ADAS pipeline, from sensor input to actuation.

2.4.1 Definition of "Closed-Loop Simulation"

In a *closed-loop* setup the simulator, the perception-planning software, and the virtual vehicle continuously feed one another:

1. The simulator renders camera (and other sensor) frames for the current moment in the scene.
2. Those frames are processed by the *real* vision stack and decision module exactly as they would be in a test car.
3. The resulting steering, throttle, and brake commands are sent back to the simulator, which moves the ego vehicle accordingly before generating the next set of frames.

Because every action produced by the software immediately influences what the sensors "see" next, the loop is *closed*. This contrasts with *open-loop* or "offline" replay, where recorded frames are simply analysed on a desktop PC and the outputs are *not* applied to the vehicle model, so the software never experiences the consequences of its own decisions.

This fidelity study relies on the closed-loop property: only when the controllers steering and braking commands are reapplied to the virtual car can observations be made about how different rendering qualities propagate through the whole perceive-decide-act chain and alter metrics of interest.

2.5 Performance-Evaluation Metrics

Closed-loop fidelity experiments require metrics that move *continuously* with perception quality, not merely pass/fail flags which could miss pinpointing subtle changes in results. Three variables—chosen for their prevalence in the AEB and lane-keeping literature and for the ease with which they can be extracted from our simulation tests—are the quantities we measure in all experiments:

t_{AEB} : Simulation time at AEB activation (ms; logged in ns)

d_{AEB} : Distance to lead object at AEB activation (m)

TTC_{AEB} : Time-to-Collision at AEB activation (s)

2.5.1 AEB Activation Time t_{AEB}

Euro New Car Assessment Programme (Euro NCAP; hereafter NCAP) defines AEB activation time (t_{AEB}) as the instant the system initiates autonomous braking [12]. Formally, this is determined by identifying the last time point where the vehicles longitudinal (forward-direction) acceleration drops below -1 m/s^2 , and then tracing back to the point where it first crossed below -0.3 m/s^2 . This method captures the moment just before the braking action meaningfully begins.

The simulation advances with a fixed $\Delta t = 25$ ms (2.5×10^7 ns in logs). Activation time t_{AEB} is recorded at the first step where the AEB trigger is set and *reported in milliseconds*. Since our simulation provides exact ground-truth control signals, we avoid relying on filtered acceleration and instead use the systems internal AEB trigger point as t_{AEB} .

2.5.2 Distance to Lead Object at AEB Activation d_{AEB} (longitudinal)

To reflect the forward collision geometry, we define distance along the road/ego vehicle longitudinal axis. Let $\hat{\mathbf{s}}(t) \in \mathbb{R}^3$ be the ego vehicles longitudinal unit vector at time t (e.g., the road-tangent in the OpenDRIVE s -frame from Sec. 2.2.1, or equivalently the ego vehicles forward heading in world coordinates). Define the signed longitudinal gap

$$g_{\parallel}(t) = (\mathbf{p}_{\text{lead}}(t) - \mathbf{p}_{\text{ego}}(t))^{\top} \hat{\mathbf{s}}(t).$$

We report

$$d_{AEB} = g_{\parallel}(t_{AEB}).$$

When OpenDRIVE arc-length coordinates are available, this is equivalent to $d_{AEB} = s_{\text{lead}}(t_{AEB}) - s_{\text{ego}}(t_{AEB})$. In our scenarios the lead object is ahead at activation, so $d_{AEB} \geq 0$.

2.5.3 Time-to-Collision at AEB Activation TTC_{AEB} (longitudinal)

We likewise compute TTC using the *longitudinal closing speed*. Let

$$v_{\text{rel},\parallel}(t) = (\mathbf{v}_{\text{ego}}(t) - \mathbf{v}_{\text{lead}}(t))^{\top} \hat{\mathbf{s}}(t),$$

so that $v_{\text{rel},\parallel} > 0$ indicates the ego vehicle is closing the longitudinal gap. Then

$$\text{TTC}_{AEB} = \begin{cases} \frac{g_{\parallel}(t_{AEB})}{v_{\text{rel},\parallel}(t_{AEB})}, & \text{if } v_{\text{rel},\parallel}(t_{AEB}) > 0, \\ \text{undefined}, & \text{otherwise.} \end{cases}$$

With OpenDRIVE s -coordinates this reduces to the familiar 1D form $\text{TTC}_{AEB} = \frac{s_{\text{lead}} - s_{\text{ego}}}{\dot{s}_{\text{ego}} - \dot{s}_{\text{lead}}}$ evaluated at t_{AEB} , defined only when $\dot{s}_{\text{ego}} > \dot{s}_{\text{lead}}$.

2.5.4 Alignment with Safety Standards

While this study primarily uses timing-based metrics such as AEB activation frame and Time-to-Collision (TTC) to evaluate system performance, these metrics are also relevant to broader safety validation frameworks.

The ISO/PAS 21448 standard, also known as Safety of the Intended Functionality (SOTIF), emphasizes the need to test not only for functional correctness but also

for system behaviour in insufficiently specified or unknown conditions [13]. This is particularly relevant for ADAS perception systems, which can behave unpredictably under unusual lighting, occlusion, or scene clutter.

In parallel, NCAP has outlined ambitions to incorporate simulation into future safety assessments [14]. Their Roadmap 2030 includes increased reliance on digital twins and scenario-based testing, where visual realism plays a crucial role in evaluating system robustness.

These developments support the importance of high-fidelity simulation as explored in this thesis. By evaluating system behaviour under varied visual conditions, simulation-based testing can help identify perception limitations earlier in the development cycle and contribute to safer ADAS deployment.

2.6 Core Perception Module: Zenseact DLOD

Zenseact DLOD (deep learning object detection) is a *single-frame* monocular detector built on the open-source Fully Convolutional One-Stage 3D (FCOS3D) framework [15]. In FCOS3D, every rendered frame is passed through DLOD to yield a list of 3-D objects—class, position, size, yaw, depth and ground-plane velocity—that a downstream tracker smooths over time.

2.6.1 Why FCOS3D?

FCOS3D extends the 2-D Fully Convolutional One-Stage (FCOS) family of anchor-free, fully convolutional detectors [16]. Instead of sliding thousands of hand-tuned "anchor" boxes across the image, every pixel in a multi-scale feature pyramid can vote for an object if it lies near that object's projected centre. This technique, among others, has led FCOS3D to achieve 1st place out of all vision-only methods in the nuScenes 3D detection challenge of NeurIPS 2020 [15], making it a solid base for any perception-based tasks.

2.6.2 Key Design Choices

- **Anchor-free voting.** Fewer hyper-parameters and better recall for very small or very large objects than anchor-based designs.
- **Scale-aware pyramid.** Objects are routed to the appropriate feature-pyramid level by simple 2-D size rules.
- **Gaussian centre-ness.** A 2-D Gaussian quality score down-weights low-confidence detections before non-maximum suppression [15].
- **Distance-based assignment.** When boxes overlap, the sample point is assigned to the object whose projected centre is nearest, boosting recall for large actors such as buses and trailers.

2.6.3 Performance

On the public nuScenes camera-only benchmark FCOS3D reaches a *mean Average Precision* (mAP) of 0.358 and a *nuScenes Detection Score* (NDS) of 0.428. NDS is the headline metric for the dataset; it blends mAP with five true-positive quality terms—translation (ATE), scale (ASE), orientation (AOE), velocity (AVE) and attribute (AAE) errors—so a higher score means both good classification and well-shaped 3-D boxes. These figures exceed the open-source CenterNet baseline while requiring roughly one third of the training time [15].

Strengths include accurate yaw estimation and strong precision on small objects such as traffic cones and barriers. Weaknesses are depth over-estimation of distant large vehicles and missed detections under heavy occlusion.

2.7 Game-Engine Rendering Pipelines

This section gives a short description of the two game engines Unity and UE5 by mentioning core rendering technologies used.

2.7.1 Unity URP (Low-Fidelity Baseline)

Unity’s Universal Render Pipeline emphasises forward lighting and single-bounce shadows [5]. Frame time scales roughly linearly with pixel count; global illumination is approximated via pre-computed light-maps [17]. Such choices typically yield real-time performance even on embedded or mobile hardware [18], but omit multiple-scattering, spectral reflections and sensor high-dynamic-range artifacts.

2.7.2 Unreal Engine 5 + Lumen/Path Tracing (High Fidelity)

Unreal Engine 5 (UE5) introduces hardware-accelerated Nanite meshes (see section 2.7.2.2) and the Lumen real-time global-illumination (GI) system [19]. For offline export, the built-in Path Tracer provides unbiased lighting, area shadows and spectral reflections [20].

2.7.2.1 Why UE5 for the fidelity sweeps

This study requires (i) scalable scene enrichment and (ii) controllable, physically-based lighting that can be varied per run without light baking. UE5 satisfies (i) via Nanite (virtualized geometry with fine-grained streaming and automatic LOD) together with the PCG framework for fast forest/roadside generation; and (ii) via Lumen, which supplies dynamic global illumination and soft shadowing.

2.7.2.2 Nanite Virtualized Geometry

Nanite encodes meshes as a hierarchy of cluster tiles that are streamed to the graphics processing unit (GPU) only when visible. This virtualised rasterisation removes

manual level-of-detail (LOD) creation and keeps frame cost proportional to on-screen pixel coverage [21].

2.7.2.3 Lumen Dynamic Global Illumination

Lumen gathers direct lighting in screen space, injects it into a signed-distance-field surface cache, and traces diffuse and specular bounces using a hybrid of screen-space and hardware ray tracing, depending on GPU capability. The cache is updated each frame, enabling fully dynamic GI without requiring baked lightmaps [22].

As shown in Figure 2.3, Lumen is capable of simulating advanced lighting effects such as colour bleeding and soft indirect shadowing in real time. These effects enhance scene richness and photometric realism, contributing to more challenging and representative conditions for perception stacks.



Figure 2.3: Demonstration of Lumen global illumination in UE5.

2.7.2.4 Theoretical Expectations

These features make it straightforward to manipulate shadows, sky/atmosphere, sun elevation and azimuth, and scene clutter at scale, which are more difficult to reproduce in our Unity setup. This allows controlled *fidelity variations* (lighting/shadows, sky and sun position, procedural scene structure) that alters image statistics—contrast, illumination patterns, occlusions, and local textures without changing scenario logic.

Prior work shows convolutional neural network (CNN) predictions are sensitive to such shifts [23] and often rely on texture cues [24]. We therefore expect UE5-driven fidelity changes to affect intermediate features, detector confidence, and processing latency. In a closed loop, even small shifts move the AEB threshold-crossing time, potentially advancing, delaying, or suppressing the intervention and thus changing t_{AEB} , d_{AEB} , and TTC_{AEB} .

2. Theory

3

Methods

To produce the data needed for this fidelity study, developing a system capable of running closed-loop tests was necessary. This chapter aims to provide descriptions of the different parts of this simulation loop and how their communication is set up. It also lists the scenarios tested in the two fidelity levels, along with methods used to obtain and analyze the data.

3.1 Architecture overview

A lightweight *orchestration container* starts three processes: `esmini`, UE5 and Zenseacts vision stack. From this point on, we refer only to those programs themselves:

1. **Fixed-step advancement** – `esmini` advances the scenario in fixed simulation steps. For each step it computes and updates the positions and rotations of moving objects based on the *previous steps* control outputs from the vision stack.
2. **State propagation to the renderer.** The updated actor states and the current simulation timestamp are provided to the game engine (UE5). The engine applies these states to the scene for the same step.
3. **Image acquisition** – UE5 renders the camera frame corresponding to that step and forwards the image to Zenseacts vision stack.
4. **Perception and decision** – The vision stack analyses the frame and outputs control decisions (e.g., brake, maintain speed, change lane). These decisions constitute the control signals for the next simulation step.
5. **Actuation application** – On the subsequent step, `esmini` applies the received control signals, advances the world state accordingly, and the cycle repeats.
6. **Time synchronization** – All components are aligned by the step index and simulation timestamp supplied by `esmini`. Preserving this ordering and these timestamps ensures determinism and repeatability.

3.1.1 Implemented Software Components

To realise the closed loop and enable controlled fidelity variations, we implemented:

- **FIFO-based inter-process communication (IPC) and message schema:** a per-step request/acknowledgement protocol (*tick-tock*) between `esmini` and UE5, with `TickMessage` (poses/IDs, t_k , Δt) and `TockMessage` (acknowledgment) (§3.2).
- **`esmini` runner:** the `EsminiRunner::Step()` loop that collects dynamic ground truth, sends `TickMessages`, waits for the `TockMessage`, and advances the logical time (3.4).
- **UE5 integration:** a `GameInstance`-based module with pre/post frame hooks to apply per-step state, capture and forward images to the vision stack, and send the `TockMessage` (3.3).
- **Scene construction & configuration:** an OpenDRIVE road-mesh builder and a small configuration layer to toggle visual factors (e.g., procedural clutter) (3.6.1, 3.6.2).
- **Camera capture & streaming:** render-target readout and step-aligned frame streaming to the vision stack (3.6.3, 3.7).

3.2 Inter-Process Communication

A pair of FIFOs (first in first out, also called named pipes—one method of IPC in Linux) [25] implement a per-step request/acknowledgement protocol (*tick-tock*) between `esmini` and UE5 to ensure determinism and consistency: *Tick* = step state from `esmini` to UE5 (updated poses + timestamp); *Tock* = UE5s acknowledgement for the same step after rendering; `esmini` advances only after the Tock.

Table 3.1: FIFOs used for synchronization.

FIFO path	Direction	Payload struct
/tmp/myfifo	<code>esmini</code> → UE5	<code>TickMessage</code>
/tmp/myfifo2	UE5 → <code>esmini</code>	<code>TockMessage</code>

Furthermore, UE5 transfers data to Zenseact over a Transmission Control Protocol (TCP) socket, which is another means of IPC similar to named pipes, over the network [26].

3.2.1 Message layout

This section specifies how processes exchange data along the simulation timeline. Two named pipes (FIFOs) implement request/acknowledgement handshake between `esmini` and UE5: `esmini` sends the step state; UE5 acknowledges after rendering

and dispatch. In parallel, UE5 forwards the rendered image to the vision stack over a socket (ZeroMQ (ZMQ)/TCP). The goal is to bind every data item (actor states, images, control signals, logs) to a unique step index and simulation timestamp.

```

/* Tick Message Format */
#define TRANSFORM_NAME_MAX_SIZE 64
#define TRANSFORM_BATCH_COUNT    32

struct Vec3 { float x, y, z; };
struct Transform {
    char name[TRANSFORM_NAME_MAX_SIZE];
    Vec3 Position;           // metres (OpenSCENARIO world)
    Vec3 Orientation;        // roll, pitch, yaw in rad
    int ID;                  // OpenSCENARIO object ID
};

/* esmini -> UE5 */
struct TickMessage {
    uint64_t step;           // simulation step index (monotonic)
    int64_t time_ns;         // simulation time since start [ns]
    float deltaTime;         // t since previous frame [s]
    int count;               // number of valid transforms
    bool isLastMessage;      // multi-packet support
    Transform transformsBuffer[TRANSFORM_BATCH_COUNT];
};

/* UE5 -> esmini */
struct TockMessage {
    uint64_t step;           // echoed step index
    int64_t time_ns;         // echoed simulation time [ns]
};

/* UE5 <-> Zenseact */
struct Trigger { uint8_t value; }; // handshake signal
struct Image_Data{
    struct Header {
        int32_t image_size_bytes; // payload size
        int64_t time_ns;          // simulation time [ns]
        uint64_t step;            // step index
    } header;
    std::vector<uint8_t> image_data; // RGBA bytes
};

```

Listing 1: Message layout

3.3 UE5 endpoint

The UE5 endpoint applies `esmini`'s step state to the scene, renders the corresponding camera frame, ships the image to the vision stack, and then acknowledges the

3. Methods

step back to `esmini`. The `GameInstance` initializes the pipes during startup and registers two frame-bracketing delegates: a pre-render hook (`OnPreTick`) to receive and apply transforms, and a post-render hook (`OnPostTick`) to dispatch the image and send the acknowledgement.

3.3.1 Init

At startup, UE5 opens the FIFO endpoints (incoming step state, outgoing acknowledgement) and registers the pre/post frame delegates. This establishes the communication pipes used by the handshake.

```
void UMyGameInstance::Init()
{
    Super::Init();

    OnPreTickHandle =
        FWorldDelegates::OnWorldTickStart.AddUObject(
            this, &UMyGameInstance::OnPreTick);
    OnPostTickHandle =
        FWorldDelegates::OnWorldPostActorTick.AddUObject(
            this, &UMyGameInstance::OnPostTick);

    tickPipe = open("/tmp/myfifo", O_RDONLY); // esmini -> UE5
    tockPipe = open("/tmp/myfifo2", O_WRONLY); // UE5 -> esmini
    check(tickPipe != -1 && tockPipe != -1);
}
```

Listing 2: Init

3.3.2 Pre-tick — receive updated poses

Before rendering a frame for each step, UE5 *blocks* on the inbound FIFO, receives the step state from `esmini`, validates the step index/timestamp, and applies the provided transforms to scene actors. This guarantees that the rendered frame reflects exactly the world state computed by `esmini`.

```
void UMyGameInstance::OnPreTick(UWorld*, ELevelTick, float)
{
    TickMessage msg{};
    ReadBlocked(tickPipe, &msg, sizeof(msg));

    // Cache for echo in PostTick
    LastTickStep = msg.step;
    LastTickTimeNs = msg.time_ns;

    for (int i=0; i<msg.count; ++i) {
        const auto& T = msg.transformsBuffer[i];
        const FTransform UE5 =
            CoordTranslate::OdrToUnreal::ToTransform(
                T.Position, T.Orientation);
        UpdateOrSpawnActor(T.ID, FString(T.name), UE5);
    }
}
```

Listing 3: Pre tick

3.3.3 Post-tick —broadcast data to other processes

After rendering the frame for the current step, UE5 forwards the image to the vision stack and then sends an acknowledgement back to `esmini`. The acknowledgement signals that image production/dispatch for the step has completed, allowing `esmini` to advance to the next step. Ordering and timestamp equality provide the synchronization guarantee.

```
void UMyGameInstance::OnPostTick(UWorld*, ELevelTick, float)
{
    CaptureAndLog();

    TockMessage tm{ LastTickStep, LastTickTimeNs };
    WriteBlocked(tockPipe, &tm, sizeof(tm));
}
```

Listing 4: Post tick

3.4 `esmini` endpoint

`esmini` keeps track of the simulation steps. At each step, it collects ground truth, computes updated positions and orientations for moving objects, sends this information to UE5, and *blocks* until UE5 returns an acknowledgement for the same timestamp. After the acknowledgement, `esmini` advances the logical simulation

time and applies the control outputs from the vision stack on the next step. This fixed-step, acknowledged progression ensures determinism and comparability across runs.

```
bool EsminiRunner::Step()
{
    osi3::GroundTruth gt;
    CollectDynamicGroundTruth(gt);

    int start = 0;
    while(start < gt.moving_object_size()){
        TickMessage t{};
        start = CreateMessage(t, gt, start);
        WriteBlocked(tickPipe, &t, sizeof(t));
    }

    TockMessage tk{};
    ReadBlocked(tockPipe, &tk, sizeof(tk));
    logical_time_ = tk.time;

    return ++current_step_ < nr_of_steps_;
}
```

Listing 5: esmini endpoint

3.5 Timing and Determinism

UE5 waits for Zenseact's trigger byte *inside* the `OnPostTick` event, after the current frame has executed, so the presence of the vision stack cannot disturb determinism. Furthermore, there is a timeout mechanism for this process. When the time runs out, UE5 simply skips sending the data and proceeds to the next step, guaranteeing determinism.

3.6 Scene construction and coordinate systems

The visual world is built at run-time by two subsystems:

1. **Road-mesh tessellation**: converts OpenDRIVE centre-lines into triangle meshes, creating the road (3.6.1);
2. **Procedural content generation (PCG)**: generates vegetation (3.6.2);

3.6.1 Road-mesh builder

Road geometry is generated by the function in Listing 6. OpenDRIVE metre-based, right-handed coordinates (x, y, z) [m] are mapped to Unreal's left-handed, centimetre-based coordinates by $(x, y, z)_{UE5} = (+100x, -100y, +100z)$. (Note that these coordinates are scaled up by a factor of 100, metre-based to centimetre-based).

```
void FRoadMeshBuilder::BuildMesh(UWorld* W,
                                  const odr::Mesh3D& M,
                                  FString Name,
                                  FString Mat,
                                  float Zlift)
{
    TArray< FVector> UEverts; UEverts.Reserve(M.vertices.size());
    for(const auto& v : M.vertices){
        FVector P = CoordTranslate::OdrToUnreal::ToLocation(v);
        P.Z += Zlift;
        UEverts.Add(P);
    }

    UProceduralMeshComponent* PM =
        NewObject<UProceduralMeshComponent>(W->GetWorldSettings());
    PM->RegisterComponent();
    PM->CreateMeshSection(0, UEverts,
                          ToUE(M.indices),
                          UpNormals(UEverts),
                          ToUV(M.st_coordinates),
                          {}, {}, true);
    PM->SetMaterial(0, LoadObject<UMaterialInterface>(nullptr,*Mat));
}
```

Listing 6: Road mesh builder

3.6.2 Procedural generation

UE5's PCG system generates spawn points for vegetation to be created at. The meshes are Nanite-based, making it possible for the system to handle a big amount of generated meshes. These are generated inside a **BoxComponent** that is created around the road. Density and seed are set at run-time:

3. Methods

```
PCGComponent->GetGraphInstance()
    ->SetGraphParameter<float>("NewProperty",
        0.01f); // density
PCGComponent->GetGraphInstance()
    ->SetGraphParameter<float>("NewProperty_1",
        Seed); // seed
```

Listing 7: Procedural generation

3.6.3 Camera setup

A Volvo JavaScript Object Notation (JSON) file lists every camera's local pose, render-target size, crop window and optical centre. `AEgoCarManager` spawns one `AEgoCarCameraActor` per entry.

```
EgoCam->InitializeCamera(ConvertedPos,
    ConvertedRot,
    DestSize, Crop, Center,
    EEgoCarImageLog::PNGLogger);
```

Listing 8: Camera setup

Each capture follows Listing 9.

```
/* AEgoCarCameraActor::CaptureAndLog() */
SceneCaptureComp->CaptureScene();
FlushRenderingCommands(); // wait for GPU
TArray<FColor> Raw;
UKismetRenderingLibrary::ReadRenderTarget(this,
    RenderTarget,
    Raw,
    false);
ProcessCapturedImage(Raw, Crop);
ZmqSocket->send(Crop.GetData(), Crop.Num()*4);
ZmqSocket->recv(); // wait
```

Listing 9: Virtual image capture

3.7 Synchronous image loop

Figure 3.1 illustrates the deterministic three-party handshake.

1. The container sends updated actor positions/orientations together with the step index and timestamp to UE5 via `/tmp/myfifo`. UE5 blocks in `ReadBlocked()` until the state is available.

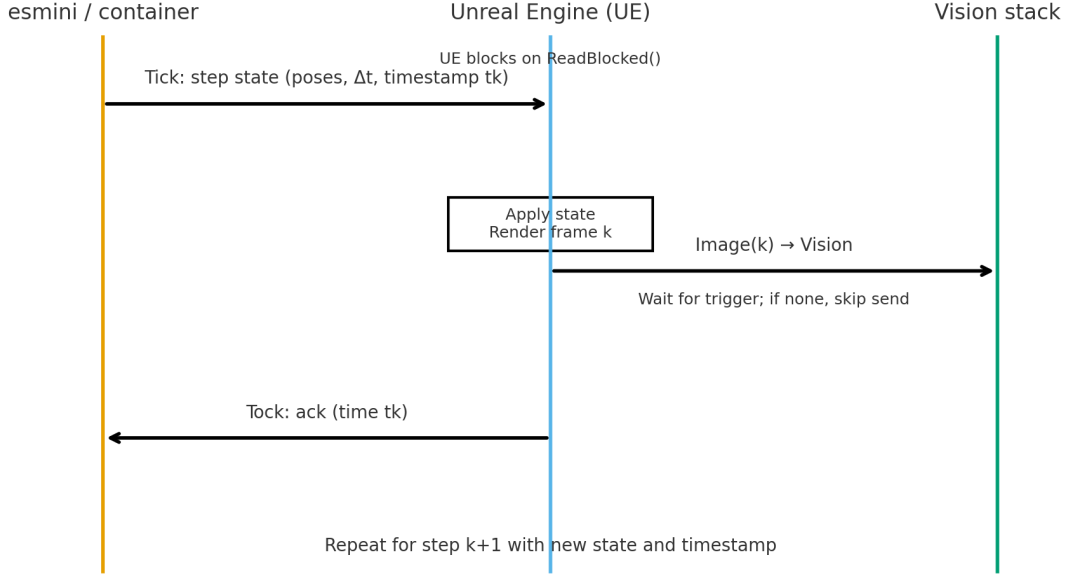


Figure 3.1: Per-step synchronization between `esmini`, UE5, and the vision stack. `esmini` sends the step state (Tick), UE5 renders and conditionally ships the image to the vision stack, then acknowledges the same step (Tock).

2. UE5 applies the received state, renders the camera frame for the same step, waits for the trigger byte on the socket, and—if triggered—sends the image to the vision stack. If the trigger does not arrive in time, sending is skipped for that step.
3. UE5 writes an acknowledgement with the (same) step index/timestamp to `/tmp/myfifo2`. The container blocks in `ReadBlocked()` and reads the acknowledgement to confirm synchronization before advancing to the next step.

3.8 Game-Engine Alignment

To increase the likelihood that any behavioural differences originate from the difference in visual fidelity between Unity and UE5, the following aspects are kept as identical as practical across both pipelines:

- **Road network and traffic logic** — Identical OpenDRIVE maps and OpenSCENARIO storyboards are parsed by `esmini` and streamed, step-for-step, to the two renderers. The pedestrians and vehicles are therefore kept in the same position and orientation at simulation step k .
- **Sensor model** — The virtual camera inherits the same resolution, crop window and fisheye lens distortion. Exposure adaptation is disabled in both engines.
- **Actor appearance** — The car and pedestrian meshes were imported unchanged, and their materials were manually re-created in UE5 using the same

albedo, normal-map and metallic-roughness textures as in the Unity pipeline. Because the two engines employ different shading models, minor visual differences may remain, but every effort was made to match colors and gloss levels as closely as possible.

- **Simulation clock** — `esmini` remains the single source of time (Sec. 3.5), issuing a fixed Δt Tick. Unity and UE5 render a new frame only after receiving that Tick, thereby sampling the simulation on an identical timeline.
- **Image I/O path** — Images are transferred to the Zenseact perception stack over an identical TCP socket and logged using the Hierarchical Data Format version 5 (HDF5) schema described in Sec. 3.10.

The goal of keeping these aspects identical is to keep the renderer as the sole experimental variable. Any statistically significant shift in the closed-loop metrics should therefore originate from a change in fidelity.

3.8.0.0.1 Motivation for the cross-engine baseline check. Because our scenarios and assets are exported from Unity to UE5 (identical OpenDRIVE/OpenSCENARIO logic; matched camera intrinsics; re-created materials), we first test whether any *inherent* engine differences would bias results. We therefore compare Unity-URP to UE5 with all fidelity features disabled and summarize paired differences per scenario. Only after establishing close agreement do we analyze fidelity factors—strictly within UE5—to isolate lighting and scene-complexity effects from cross-engine confounds.

3.9 Experimental Scenarios

We use a partially crossed factorial design in UE5 to isolate how visual phenomena influence perception and control. Starting from the UE5 baseline (plain white sky, no shadows, no environmental enrichment), three primary fidelity factors are explored (see Table 3.2):

Table 3.2: Visual-fidelity factors explored in UE5

Factor	Levels
(1) Environmental clutter (PCG-scattered trees, saplings, tall grass & rocks)	Off
	On
(2) Skybox	Off (plain white, Unity baseline)
	On (blue sky with volumetric clouds)
(3) Shadows	Off
	On

Figure 3.2 illustrates the effect of enabling each of the three fidelity factors, using consistent scene geometry and camera angle. Shadows, when shown, use a zenith sun (90° elevation).

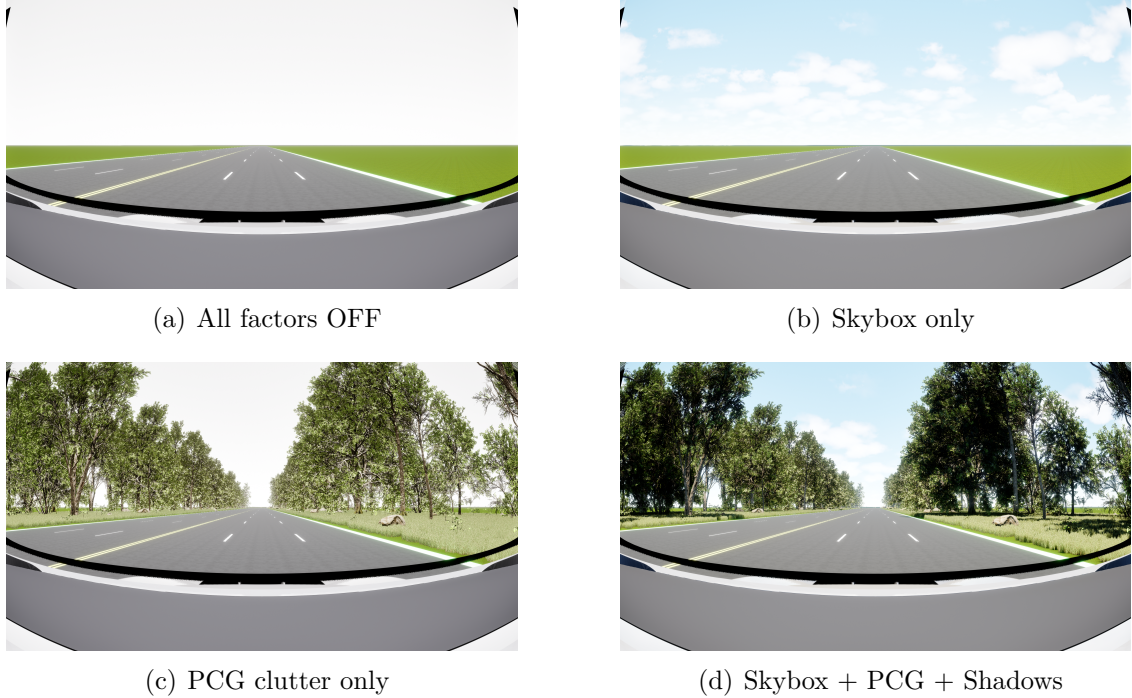


Figure 3.2: Effect of enabling each of the three fidelity factors. Shadows use a zenith sun (90° elevation) in all images.



Figure 3.3: Effect of sun elevation angle on lighting and shadows, with sun fixed in the west. From left to right: 90° (zenith), 45°, and 10° above the horizon. Lower sun angles produce longer, softer shadows and warmer lighting effects.

Table 3.3: Sun-light directions tested when *shadows = On*

Label	Cardinal direction	Elevation
S ₀	Zenith (straight up)	90°
S _{1-S₄}	N, E, S, W	45°
S _{5-S₈}	N, E, S, W	10°

3. Methods

The lower the sun is above the horizon, the more extreme the shadows cast by objects in the scene are. Two different elevations are therefore tested (45° , 10°), each combined with all four cardinal directions, giving the 9 lighting directions listed in Table 3.3.

In all simulations, cardinal directions are defined relative to the ego vehicles initial orientation. Specifically, "north" is aligned with the ego vehicles forward (driving) direction, "east" points to the right, "west" to the left, and "south" behind the vehicle. This convention is used to consistently interpret the effect of sun angle and shadow orientation in all scenarios. Figure 3.3 visualizes the westward case across those elevations and the resulting changes in lighting and shadow length.

Unity remains fixed in its default configuration and serves as a baseline for comparison. The total number of UE5 test conditions is derived as follows:

- **Shadows = Off:** Only the environmental clutter and skybox toggles are relevant. The 2×2 combinations of these two binary factors yield $2^2 = 4$ conditions.
- **Shadows = On:** Lighting direction now enters. The 9 sun positions listed in Table 3.3 are each paired with the same four clutter/skybox settings, giving $9 \times 2^2 = 36$ further conditions.

$$4 \text{ [shadows off]} + 36 \text{ [shadows on]} = 40 \text{ UE5 configurations}$$

We compare the 40 UE5 configurations to one another and use the Unity build as a single baseline reference.

3.9.1 NCAP-derived Safety Scenarios

Each rendering configuration is run in eight traffic scenarios based on two Euro NCAP Automated Emergency Braking protocols: four car-to-car cases (*AEB car-to-car (C2C) v4.3.1* [12]) and four vulnerable-road-user cases (*AEB vulnerable road user (VRU) v4.5.1* [27]). Each scenario is presented with two different initial conditions. Table 3.4 lists the scenarios with their NCAP reference start conditions. All scenarios follow right-handed traffic conventions, as used in European road systems. The ego vehicle drives on the right side of the road, and pedestrian and vehicle interactions are oriented accordingly.

Table 3.4: NCAP scenarios and initial conditions

Short name	Initial conditions
Car-to-Car front turn across path	Ego 20 km/h, target 45 km/h
Car-to-Car front turn across path	Ego 20 km/h, target 60 km/h
Car-to-Car Rear braking	Ego 50 km/h, target 50 km/h (decelerate 6 m/s ²)
Car-to-Car Rear braking	Ego 50 km/h, target 50 km/h (decelerate 2 m/s ²)
Car-to-Car Rear moving	Ego 50 km/h, target 20 km/h
Car-to-Car Rear moving	Ego 80 km/h, target 20 km/h
Car-to-Car Rear stationary	Ego 50 km/h, target 0 km/h
Car-to-Car Rear stationary	Ego 80 km/h, target 0 km/h
Car-to-Pedestrian Far-side Adult	Ego 50 km/h, target 8 km/h
Car-to-Pedestrian Far-side Adult	Ego 60 km/h, target 8 km/h
Car-to-Pedestrian Longitudinal Adult	Ego 50 km/h, target 5 km/h
Car-to-Pedestrian Longitudinal Adult	Ego 80 km/h, target 5 km/h
Car-to-Pedestrian Near-side Adult	Ego 50 km/h, target 5 km/h
Car-to-Pedestrian Near-side Adult	Ego 60 km/h, target 5 km/h
Car-to-Pedestrian Near-side Child Obstructed	Ego 50 km/h, target 5 km/h
Car-to-Pedestrian Near-side Child Obstructed	Ego 60 km/h, target 5 km/h

8 scenarios \times 2 initial conditions \times 40 UE5 configurations +16 Unity baselines
 \Rightarrow 656 closed-loop runs.

3.10 Data Gathering and Processing

Running a full closed-loop test generates timestamped outputs from Zenseact’s perception and control stack. Each run is logged as an Hierarchical Data Format version 5 (HDF5) file (.hdf5) with a hierarchical structure per signal stream. One HDF5 file corresponds to one simulator run under a specific *scenario* and *rendering variant*.

3.10.1 Signals and derived metrics.

For this fidelity study we extract the following signals (time-series) from the controller logs:

- Automated Emergency Braking (AEB) state and trigger.
- Time to Collision (TTC).
- Distance to Lead Object (d_{AEB}).

Raw data are read with Python’s `h5py`, converted to `NumPy` arrays, and optionally visualised with `matplotlib`. From these signals we compute per-run metrics. The primary analysis (Section 3.11) uses Time-to-Collision at activation TTC_{AEB} (s), distance at activation d_{AEB} (m), and a non-activation indicator $\mathbb{1}_{\text{no-AEB}}$ (defined as 1 if no trigger is observed, 0 otherwise).

3.10.2 Scenario Identifiers

Each run carries a compact scenario code of the form

```
<scenario_code>_speed_<v> or <scenario_code>_decel_<a>.
```

Examples include `ccrm_speed_50`, `ccrs_speed_80`, `ccrb_decel_2`, and `cpnco_speed_60`. These uniquely identify the traffic/manoeuvre configuration and are consistent across simulators.

3.10.3 Low vs. High Fidelity Mapping

Low fidelity (UE5 “fidelity-off”): no shadows, no procedural content, zenith sun, white sky.

High fidelity (UE5 “fidelity-on”): any configuration enabling shadows and/or PCG and/or non-zenith sun angles/directions and/or a cloudy sky.

3.10.4 Cross-Simulator Baselines

For each scenario we also have one Unity baseline run. In the statistics (Section 3.11) we check alignment between Unity and UE5 *fidelity-off*.

3.11 Statistical Analysis

3.11.1 Decompose the Research Questions

To address our two research questions (RQ), we break each into testable sub-questions that map directly to the analysis below.

RQ1: Does increased simulation fidelity change ADAS behaviour?

1. **Baseline agreement (cross-simulator):** Are Unity and UE5 *fidelity-off* in agreement across scenarios for d_{AEB} and TTC_{AEB} ?
2. **Fidelity effects on continuous outcomes (within-UE5):** *How do specific fidelity factors change d_{AEB} (m) and TTC_{AEB} (s)?*

RQ2: Can higher fidelity expose hidden failure modes?

1. **Failure exposure:** Identify scenarios where Unity activates but at least one UE5 *fidelity-on* run does not.
2. **Failure predictors:** Model the association between fidelity factors and non-activation.

3.11.2 Analyzed metrics

Each run contributes two continuous metrics and one binary flag:

- TTC_{AEB} (s): Time-to-Collision at activation.

- d_{AEB} (m): distance to obstacle at activation.
- $\mathbb{1}_{\text{no-AEB}} \in \{0, 1\}$: non-activation indicator.

3.11.3 Baseline alignment across scenarios (Unity vs UE5, fidelity-off)

Our goal is to verify that *Unity* and *UE5 with fidelity disabled* yield comparable baselines so that any effects observed later can be attributed to fidelity changes rather than to simulator differences. We therefore compare, per scenario, the same metric produced by the two simulators and summarize the paired differences. This is a descriptive, matched-pairs check of *comparability*.

3.11.3.0.1 Rationale for approach. The same scenario is executed in both simulators, so a *paired* comparison by scenario is the appropriate unit of analysis. Correlation alone can be high even with systematic offsets and therefore does not assess agreement. We summarize *paired differences* because they quantify bias and spread directly on the measurement scale. Given $n=16$ scenario-level pairs, the mean difference with a t -interval is a standard summary; the RMSE of differences complements the mean by reflecting typical magnitude.

3.11.3.0.2 Setup and pairing. For each scenario s and metric m we form the paired difference

$$\Delta_{s,m} = m_s^{(\text{UE5_off})} - m_s^{(\text{Unity})}.$$

Scenarios are treated as fixed (structured variations), not a random sample.

3.11.3.0.3 Reporting (simple matched-pairs summaries). For each metric we report: (i) the *mean paired difference* $\bar{\Delta}_m$ with a 95% t -interval, (ii) the *root mean square error (RMSE)* of the differences, and (iii) the *maximum absolute difference*. To provide a scale-free sense of magnitude, we also report the symmetric percentage difference

$$100 \times \frac{2 \left| m_s^{(\text{UE5_off})} - m_s^{(\text{Unity})} \right|}{\left| m_s^{(\text{UE5_off})} \right| + \left| m_s^{(\text{Unity})} \right|}.$$

3.11.3.0.4 Visualization. We use two standard plots:

1. **Direct comparison (scatter):** Unity values on the x -axis and UE5 (fidelity-off) values on the y -axis, with the identity line $y = x$ overlaid to visualize agreement.
2. **Difference-vs-average plot:** for each scenario, the paired difference $\Delta_{s,m}$ (vertical axis) versus the scenario average $(m_s^{(\text{UE5_off})} + m_s^{(\text{Unity})})/2$ (horizontal axis). We draw a single horizontal line at the mean difference $\bar{\Delta}_m$ to visualize any systematic offset. The plot is used descriptively to check for bias and for magnitude-dependent patterns.

3.11.3.0.5 Assumptions.

- Analyses are performed at the *scenario* level using matched pairs.
- Paired differences are assumed to be approximately normal for the reported *t*-intervals.
- Both simulators produce the same metric on the same scale, so differences are directly comparable.
- Plots and RMSE are used *descriptively* to assess bias and spread rather than for strict inferential claims.

3.11.4 Fidelity effects on continuous outcomes

To quantify how visual-fidelity factors shift continuous AEB outcomes when activation occurs, we analyze within-scenario differences relative to the per-scenario UE5 baseline (fidelity off). For scenario *s* and run *i*:

$$\Delta y_{is} = y_{is} - y_s^{(\text{base})}, \quad y \in \{d_{\text{AEB}} (\text{m}), \text{TTC}_{\text{AEB}} (\text{s})\}.$$

The baseline $y_s^{(\text{base})}$ is the canonical UE5 off-state for scenario *s* (verified for all 16/16 scenarios in our data). This within-scenario transformation removes time-invariant scenario effects before modeling (fixed-effects logic) [28].

3.11.4.0.1 Design and predictors. We include UE5 runs with successful AEB activation only (continuous metrics are undefined otherwise). Binary fidelity factors are encoded as {0, 1}: Shadow (on), PCG (on), and Sky (cloudy vs. white). Sun elevation is categorical with 90° as the reference via indicators for 45° and 10°. We exclude sun *direction* as a nuisance (blocking) factor: adding four direction indicators would inflate the parameter count with limited interpretive value and reduce power; exploratory checks showed no consistent direction effect once elevation is controlled. The linear mean model for each outcome is

$$\Delta y_{is} = \beta_0 + \beta_1 \text{Shadow}_{is} + \beta_2 \text{PCG}_{is} + \beta_3 \text{Sky}_{is} + \beta_4 \mathbb{1}\{\text{Elev} = 45^\circ\}_{is} + \beta_5 \mathbb{1}\{\text{Elev} = 10^\circ\}_{is} + \varepsilon_{is}.$$

3.11.4.0.2 Estimation and uncertainty. We fit **ridge linear regression** (L2) separately for each outcome to stabilize estimates under correlated binaries and modest signal [29]. The penalty is parameterized as $\alpha = 1/C$ with $C = 5$ (intercept unpenalized). To accommodate within-scenario dependence, we compute **scenario-level cluster bootstrap** percentile intervals: with $K = 16$ scenarios and $B = 2000$ replicates, each bootstrap sample draws K scenarios with replacement, pools all rows from the drawn scenarios, refits the ridge model, and stores coefficients. The 95% confidence intervals (CI) are the 2.5th and 97.5th percentiles of the bootstrap coefficient distribution [30], [31]. Given the small number of clusters ($K = 16$), coverage may be imperfect and intervals are interpreted cautiously.

3.11.4.0.3 Rationale. Within-scenario differencing removes time-invariant scenario effects and avoids the need for mixed-effects structure at small K . The fidelity factors are binary and partially co-occur (e.g., shadows often with non-zenith elevations), creating collinearity; ridge (ℓ_2) stabilizes estimates under such correlation and modest signal-to-noise. Scenario-level cluster bootstrapping respects within-scenario dependence by resampling entire scenarios, which is preferable to IID resampling when multiple runs nest within scenario.

3.11.4.0.4 Interpretation. Because we model Δ relative to the per-scenario baseline, coefficients are *average within-scenario shifts* when a factor is “on” versus “off,” holding other factors fixed. By convention here, negative Δd_{AEB} or $\Delta \text{TTC}_{\text{AEB}}$ implies activation occurs *closer to impact* (riskier). Estimates are associational (not causal) and conditional on activation. Because analyses are restricted to runs with activation, estimates are conditional on activation status; if the fidelity factors also influence activation, conditioning can induce selection (collider) bias. Accordingly, effects are interpreted as descriptive within-activation associations rather than population-average causal effects.

3.11.5 Failure exposure

For each scenario with Unity activation, we compute the UE5 (*fidelity-on*) failure count and rate

$$C_s = \sum_{i=1}^{n_{\text{on},s}} \mathbb{1}_i^{(\text{on})}, \quad \hat{p}_s = \frac{C_s}{n_{\text{on},s}}.$$

Uncertainty is summarized by the **Wilson score** 95% confidence interval [32]

$$\text{CI}_{\text{Wilson}} = \frac{1}{1 + \frac{z^2}{n}} \left(\hat{p} + \frac{z^2}{2n} \pm z \sqrt{\frac{\hat{p}(1 - \hat{p})}{n} + \frac{z^2}{4n^2}} \right),$$

with $z = 1.96$. We summarize uncertainty with Wilson CIs; exact tests are uninformative when any nonzero count makes p trivially small.

3.11.6 Logistic regression for failure predictors

We model the probability of an AEB non-activation in *UE5* runs as a function of visual-fidelity factors using a ridge-penalized logistic regression with scenario-level cluster bootstrap for uncertainty quantification. Ridge logistic regression is well-suited for sparse events because ℓ_2 shrinkage stabilizes estimates and reduces variance [33]. We motivate penalization further by the low events-per-variable (EPV) setting [34] and use bootstrap resampling to obtain uncertainty intervals [30].

3.11.6.0.1 Outcome and scope. Let $Y \in \{0, 1\}$ indicate failure (1 = no AEB activation, 0 = activation). We fit the model on *UE5* rows only (baseline + variants); *Unity* rows are excluded. The dataset comprises **640** observations with **15** failures (2.3%).

3.11.6.0.2 Rationale. The logistic model complements the descriptive by-factor failure rates by providing an adjusted association across factors. Events are rare (15/640; low EPV), so we apply ℓ_2 -penalization to reduce variance and use scenario-level cluster bootstrap to reflect within-scenario dependence. Because the model operates in a low-signal, low-EPV regime, we treat estimates as exploratory and report them alongside the simpler rate summaries.

3.11.6.0.3 Predictors and coding. Binary factors are coded $\{0, 1\}$: `shadow` (on/off), `pcg` (on/off), and `sky` (cloudy vs. white). Sun elevation is treated categorically with 90° as the reference level via two indicator variables for 45° and 10° . The linear predictor is

$$\text{logit } P(Y = 1 \mid \mathbf{x}) = \beta_0 + \beta_1 \text{shadow} + \beta_2 \text{pcg} + \beta_3 \text{sky} + \beta_4 \mathbb{1}\{\text{elev} = 45^\circ\} + \beta_5 \mathbb{1}\{\text{elev} = 10^\circ\},$$

where β_0 is the log-odds of failure in the reference category (all factors off, elevation = 90°) and is not interpreted substantively.

3.11.6.0.4 Estimation. With only 15 events across 5 predictors (events-per-variable ≈ 3 , below conventional EPV guidelines [34]), we stabilize estimates via ridge (ℓ_2) penalization with inverse regularization strength $C = 5.0$ (larger C implies weaker penalty) [33]. We use scikit-learns `LogisticRegression` (`penalty=12`, `solver=lbfgs`), with the intercept unpenalized and class imbalance handled via `class_weight="balanced"`, i.e., a weighted likelihood with implied weights $w_1 = \frac{640}{2 \times 15} \approx 21.3$ for failures and $w_0 = \frac{640}{2 \times 625} \approx 0.512$ for activations [35]. The objective can be written (up to package-specific scaling) as

$$\hat{\beta} = \arg \max_{\beta} \left\{ \sum_{i=1}^n w_{y_i} [y_i \log p_i(\beta) + (1 - y_i) \log(1 - p_i(\beta))] - \frac{1}{2C} \|\beta_{-0}\|_2^2 \right\},$$

where $p_i(\beta) = [1 + \exp(-\mathbf{x}_i^\top \beta)]^{-1}$, β_{-0} excludes the intercept. Ridge shrinkage biases odds ratios toward 1.0; reported ORs are thus regularized and derived from a weighted likelihood.

3.11.6.0.5 Cluster bootstrap for uncertainty. To account for within-scenario dependence (multiple variants nested within scenarios), we construct confidence intervals via a *scenario-level cluster bootstrap*. Let K be the number of observed scenarios ($K = 16$ here). For each of $B = 2000$ replicates, we sample K scenarios with replacement, pool all rows from the sampled scenarios, refit the ridge logistic model, and store coefficients. Replicates with no variation in Y (all 0 or all 1) are discarded. Point estimates are from the full-data fit; 95% CIs are the 2.5% and 97.5% percentiles of the bootstrap coefficient distribution. Because this resamples entire scenarios, the resulting intervals properly account for within-scenario clustering, though they do not correct for the regularization bias. Given the small number of clusters ($K = 16$), coverage may be imperfect and intervals are interpreted cautiously.

3.11.6.0.6 Reporting and interpretation. We report effects as odds ratios $OR_j = \exp(\beta_j)$ with bootstrap 95% CIs computed as $[\exp(\beta_{j,0.025}^{\text{boot}}), \exp(\beta_{j,0.975}^{\text{boot}})]$, applying the exponential transform to coefficient percentiles. An $OR < 1$ indicates the factor is associated with *lower* failure odds; $OR > 1$ indicates *higher* odds. All effects are *associations* conditional on the model structure and observed data; they are not causal claims. Because estimates are both regularized and obtained from a weighted likelihood, bootstrap CIs reflect cluster resampling uncertainty but do not correct shrinkage bias.

3.11.7 Robustness and exclusions

Runs with undefined continuous metrics (non-activations) are excluded from metric summaries but counted in the binary failure analysis.

3. Methods

4

Results

This chapter presents results addressing the two research questions defined in §3.11. We first validate cross-simulator baseline alignment between Unity and UE5 with fidelity disabled. We then examine per-scenario fidelity effects on AEB metrics and assess whether higher visual fidelity exposes hidden failure modes. Finally, we characterize descriptive associations between individual fidelity factors and AEB behaviour.

4.1 Data Overview

We analyzed 16 scenarios, each with one Unity baseline and 40 UE5 variants (one fidelity-off baseline and 39 fidelity-on variants). Metrics and exclusion rules follow §3.11: we analyze TTC_{AEB} (s) and d_{AEB} (m) for runs with activations and treat non-activations separately as failures. As defined in §2.5.2–§2.5.3, both d_{AEB} and TTC_{AEB} are computed strictly along the road/ego vehicle *longitudinal* axis. Across all 656 runs, we observed 15 non-activations (2.3%).

4.2 Baseline Alignment: Cross-Simulator Validation

We assessed baseline comparability between *Unity* and *UE5 with fidelity disabled* using simple matched-pairs summaries across the 16 scenarios. For each metric we report the mean paired difference $\Delta = \text{UE5}_{\text{off}} - \text{Unity}$ with a 95% t -interval ($t_{0.975, 15} \approx 2.13$), the RMSE of the differences, and the maximum absolute difference; per-scenario symmetric absolute percentage differences are also provided for scale-free context.

Table 4.1: Baseline alignment (Unity vs UE5, fidelity-off): matched-pairs summaries. $\Delta = \text{UE5}_{\text{off}} - \text{Unity}$.

Metric	Unit	n	Mean Δ	95% t -CI	RMSE	Max $ \Delta $
d_{AEB}	m	16	0.4272	[0.0495, 0.8049]	0.8084	1.711
TTC_{AEB}	s	16	0.0225	[0.0005295, 0.04447]	0.04583	0.1

4. Results

Table 4.2: Per-scenario *symmetric* absolute percentage differences for baseline alignment. Percentage difference is $100 \times \frac{2|m_s^{(\text{UE5_off})} - m_s^{(\text{Unity})}|}{|m_s^{(\text{UE5_off})}| + |m_s^{(\text{Unity})}|}$.

Scenario	$d_{\text{AEB}} (\%)$	$\text{TTC}_{\text{AEB}} (\%)$
ccftap_speed_20_45_variants	0.10	0.00
ccftap_speed_20_60_variants	5.36	2.82
ccrb_decel_2_variants	0.63	0.00
ccrb_decel_6_variants	0.11	0.00
ccrm_speed_50_variants	0.02	2.06
ccrm_speed_80_variants	1.69	1.44
ccrs_speed_50_variants	0.83	1.57
ccrs_speed_80_variants	1.57	2.86
cpfa_speed_50_variants	5.03	6.67
cpfa_speed_60_variants	5.28	6.67
cpla_speed_50_variants	0.00	0.00
cpla_speed_80_variants	1.63	1.46
cpna_speed_50_variants	0.02	0.00
cpna_speed_60_variants	7.35	8.70
cpnco_speed_50_variants	5.70	5.61
cpnco_speed_60_variants	6.08	6.06
Mean	2.59	2.87
Max	7.35	8.70

Across scenarios, UE5 (fidelity-off) yields slightly larger values on average, but the shifts are small in magnitude. The symmetric absolute percentage differences average 2.59% for d_{AEB} and 2.87% for TTC_{AEB} , with maxima of 7.35% and 8.70%, respectively (Table 4.2). Overall, typical cross-simulator differences are small (approximately 2–3%), which supports using UE5 *fidelity-off* as the per-scenario baseline for the fidelity analyses.

Figure 4.1 shows the direct comparison (scatter) plots with Unity on the x -axis and UE5 (fidelity-off) on the y -axis; points cluster around the identity line, indicating close agreement. Figure 4.2 shows the difference-vs-average plots; the small positive mean differences (solid line) and roughly constant spread with no visible trend across the measurement range indicate close baseline comparability. We therefore regard the two simulators as providing sufficiently comparable baselines, and use the UE5 fidelity-off run as the per-scenario reference in the within-UE5 fidelity analyses.

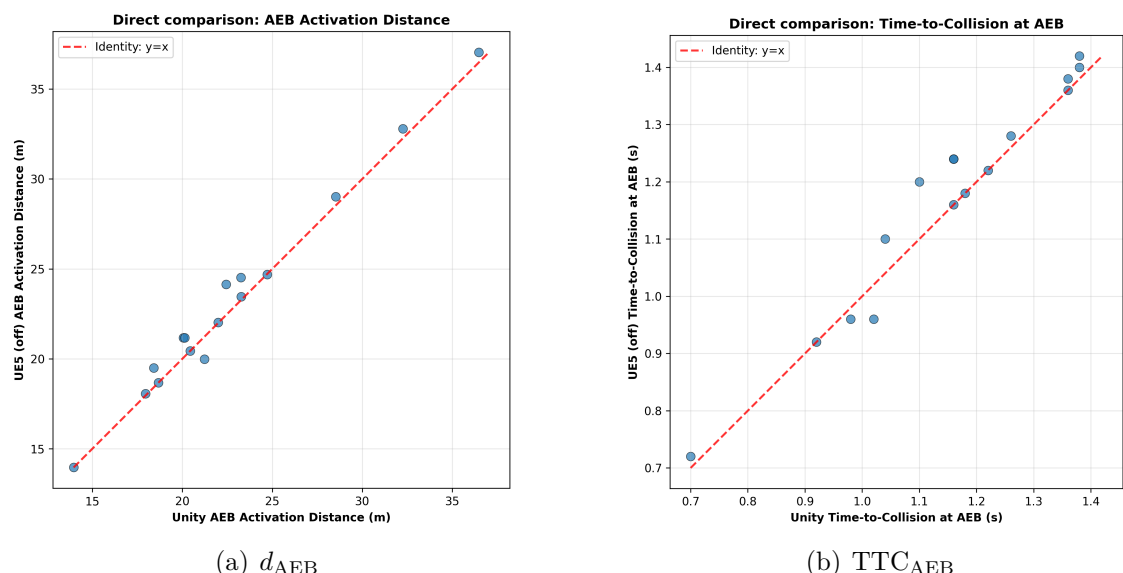


Figure 4.1: Direct comparison (scatter): Unity values (x) vs. UE5 (fidelity-off) values (y) with the identity line $y = x$. Points close to the identity line indicate strong baseline comparability.

4. Results

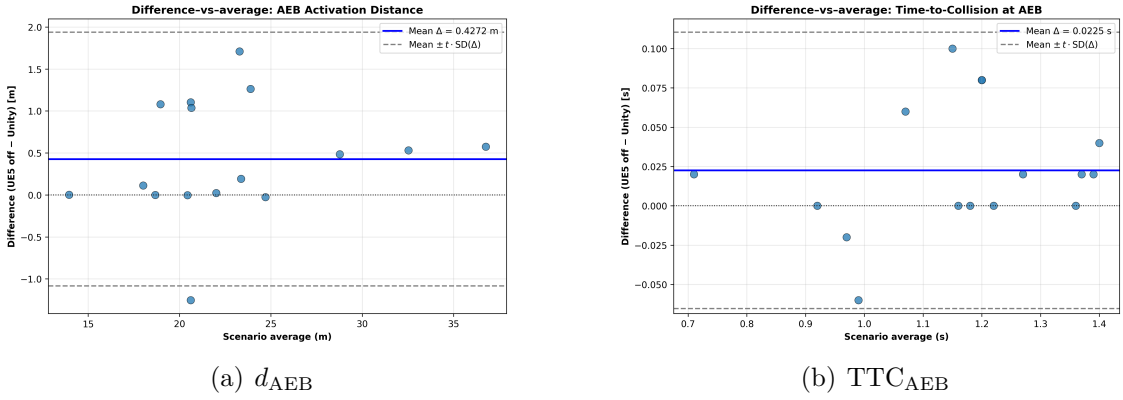


Figure 4.2: Difference–vs–average plots: per scenario, the paired difference Δ (UE5 off – Unity) is shown against the scenario average. The solid line is the mean difference $\bar{\Delta}$; dashed lines show $\bar{\Delta} \pm t_{0.975,15} \cdot \text{SD}(\Delta)$ with $t_{0.975,15} \approx 2.13$, illustrating the typical spread.

4.2.1 Fidelity effects on continuous outcomes

Across 16 scenarios, there were $N = 625$ activated UE5 runs used for the continuous-outcome analyses (all 16 baselines verified). Coefficients and scenario-cluster bootstrap 95% CIs are reported in Tables 4.3 and 4.4. By our sign convention, negative Δd or ΔTTC indicates reduced margin. Uncertainty reflects a scenario-level cluster bootstrap with $B = 2000$ replicates (degenerate draws discarded); given $K = 16$ clusters, intervals are interpreted cautiously.

A consistent pattern emerges for **low sun elevation** (10°):

- Δd_{AEB} (m): -0.963 $[-1.789, -0.349]$
- $\Delta \text{TTC}_{\text{AEB}}$ (s): -0.0535 $[-0.0936, -0.0214]$

Both intervals exclude zero and point in the same “closer” (reduced margin) direction, indicating that low sun materially erodes activation margins even when AEB still triggers.

For other factors, intervals generally include zero and effects are modest:

- **PCG(on)**: shifts toward smaller distance/TTC (e.g., $\Delta d = -0.267 \text{ m}$ $[-0.594, 0.071]$; $\Delta \text{TTC} = -0.0163 \text{ s}$ $[-0.0365, 0.0012]$) but with CIs overlapping zero.
- **Shadow(on)** and **Sky(cloudy)**: small, imprecise changes around zero across outcomes.
- **Elevation 45°**: near-null with wide CIs.

Overall, the continuous-outcome analysis suggests that *low sun elevation* is a salient fidelity condition that reduces the time/space margin at AEB activation (lower TTC_{AEB} and d_{AEB}), while other visual-fidelity features exhibit at most modest, uncertain shifts. These findings are conditional on activation and complement the failure-probability analysis in §4.3.1.

Table 4.3: Ridge linear model for Δd_{AEB} (metres); scenario-cluster bootstrap 95% CI.

Feature	Effect (CI)
Shadow (on)	-0.1676 [-0.5332, 0.1559]
PCG (on)	-0.2671 [-0.5938, 0.0711]
Sky (cloudy vs white)	0.0773 [-0.0426, 0.2020]
Elevation 45° (vs 90°)	-0.1311 [-0.4015, 0.0878]
Elevation 10° (vs 90°)	-0.9628 [-1.7893, -0.3488]

Table 4.4: Ridge linear model for $\Delta \text{TTC}_{\text{AEB}}$ (seconds); scenario-cluster bootstrap 95% CI.

Feature	Effect (CI)
Shadow (on)	-0.0113 [-0.0352, 0.0081]
PCG (on)	-0.0163 [-0.0365, 0.0012]
Sky (cloudy vs white)	0.0045 [-0.0030, 0.0125]
Elevation 45° (vs 90°)	-0.0061 [-0.0173, 0.0043]
Elevation 10° (vs 90°)	-0.0535 [-0.0936, -0.0214]

4.3 Failure Mode Exposure

We identified scenarios where Unity successfully activated AEB but at least one UE5 *fidelity-on* variant failed to activate. Table 4.5 lists the five scenarios meeting this criterion, along with failure rates and Wilson score 95% confidence intervals.

Table 4.5: Scenarios where higher fidelity exposed AEB failures (EyeCar activated successfully).

Scenario	Failures	Rate (%)	95% CI (%)
ccrb_decel_2	1/39	2.6	[0.5, 13.2]
ccrm_speed_50	2/39	5.1	[1.4, 16.9]
cpla_speed_50	8/39	20.5	[10.8, 35.5]
cpnco_speed_50	1/39	2.6	[0.5, 13.2]
cpnco_speed_60	3/39	7.7	[2.7, 20.3]

Higher visual fidelity exposed failures in 5 of 16 test scenarios (31.3%), indicating that AEB non-activations occurred selectively under increased rendering realism. Within these affected scenarios, failure rates among fidelity-on variants ranged from 2.6% to 20.5% (Table 4.5). The Wilson score 95% confidence intervals indicate the plausible range of true failure rates for each scenario. In all five cases, the baseline Unity run activated successfully, indicating **hidden vulnerabilities** revealed only when visual complexity increases.

To investigate whether particular fidelity factors systematically predict these failures

4. Results

across scenarios, we next fit a logistic regression model.

4.3.1 Logistic regression of failure on fidelity factors

We analyzed $N = 640$ *UE5* runs across 16 scenarios, of which 15 (2.3%) were non-activations. The ridge-penalized logistic model described in §3.11.6 was fit to the pooled *UE5* data, and uncertainty was quantified via a scenario-level cluster bootstrap with $B = 2000$ replicates (1,997 successful resamples; degenerate draws with no outcome variation were discarded). Estimates use ridge (ℓ_2) shrinkage with `class_weight="balanced"`; odds ratios are therefore regularized and reflect a weighted likelihood. Table 4.6 reports odds ratios (OR) with 95% cluster-bootstrap confidence intervals (CIs).

Table 4.6: Ridge-penalized logistic regression predicting AEB non-activation. Odds ratios (OR) with 95% scenario-cluster bootstrap CIs; baseline is Shadow=off, PCG=off, Sky=white, Elevation=90°.

Factor	OR (95% CI)	Significant	Direction
Shadow	2.75 [0.00, 10.90]	False	Harmful
PCG	0.17 [0.00, 0.76]	True	Protective
Sky (cloudy vs. white)	1.68 [0.14, 301.53]	False	Harmful
Elevation 45° (vs 90°)	0.19 [0.07, 18.27]	False	Protective
Elevation 10° (vs 90°)	0.17 [0.02, 49.95]	False	Protective

OR = odds ratio; CIs from scenario-level cluster bootstrap (2,000 replicates).

In this dataset, the interval for `pcg` (on vs. off) does not cover 1, indicating an association with *lower* odds of failure (OR < 1). Intervals for `shadow`, `sky` (cloudy vs. white), and the elevation indicators are wide and overlap 1. Given the small number of failures (15/640) and within-scenario dependence, these are exploratory associations rather than definitive effects. Odds ratios are regularized (ridge), which shrinks estimates toward 1; CIs reflect cluster resampling and do not correct shrinkage bias.

5

Discussion

This chapter interprets the findings of the experimental analysis and reflects on their significance for simulation-based ADAS testing. We discuss implications, limitations, and applicability to research and industrial practice, and we connect the results to methodological choices made in §3.11.

5.1 What the baseline validation establishes

Cross-simulator checks using *simple matched-pairs summaries* across the 16 scenarios show that Unity and UE5 with fidelity disabled provide closely comparable baselines. For both d_{AEB} and TTC_{AEB} , the mean paired differences are small with narrow 95% t -intervals, RMSEs are modest relative to the metric ranges, and per-scenario symmetric percentage differences average about 2–3%. Identity-line scatter plots exhibit tight clustering around $y=x$, and difference-vs-average plots show near-zero bias with no magnitude-dependent pattern. Consequently, differences observed when fidelity factors are enabled can be credibly attributed to the fidelity manipulations rather than to inherent simulator differences, and we use the UE5 *fidelity-off* run as the per-scenario baseline for within-UE5 analyses.

5.2 How fidelity changes AEB activation margins

Within-UE5 analyses condition on activation and model within-scenario deltas relative to the scenarios fidelity-off baseline (§3.11.4, §4.2.1). This fixed-effects logic removes time-invariant scenario structure and focuses inference on how visual factors shift margins when AEB does fire.

A consistent picture emerges for **low sun elevation** (10°): later activation in time and closer activation in space (negative shifts in d_{AEB} and TTC_{AEB} , positive shift in t_{AEB}), with all three 95% scenario-cluster bootstrap intervals excluding zero. Other factors (PCG, shadow, sky; and elevation 45°) show modest point shifts with intervals overlapping zero. Taken together, these results suggest that *illumination geometry*, rather than generic visual richness, is the most salient driver of margin erosion in this dataset. Importantly, the estimates are *associational* and *conditional on activation*; they quantify descriptive shifts among runs where the controller still triggers AEB.

5.3 Higher fidelity exposes hidden non-activations

Failure exposure analysis (§4.3) shows that enabling fidelity factors revealed non-activations in **5/16** scenarios (31.3%), despite successful activation in the corresponding Unity baselines. Scenario-level failure rates among fidelity-on variants ranged from 2.6% to 20.5% with Wilson 95% intervals. This is the practical headline: *higher visual fidelity can surface safety-relevant failure modes that remain invisible in low-fidelity scenes*. From a validation perspective, this argues for including fidelity sweeps in regression suites rather than relying on visually clean baselines.

5.4 Interpreting the failure model

The ridge-penalised logistic regression (§3.11.6, §4.3.1) is explicitly exploratory given the low event count (15/640). Penalisation stabilises coefficients in a low-EPV regime and `class_weight="balanced"` targets a weighted likelihood. Confidence intervals are from a scenario-level cluster bootstrap, which respects within-scenario dependence but does not undo shrinkage bias.

Within these constraints, the `pcg` coefficients 95% interval lies entirely below 1 on the OR scale (association with lower failure odds); intervals for `shadow`, `sky` and elevation indicators overlap 1. Because the analysis is pooled across heterogeneous scenarios and uses a weighted likelihood, these associations should be read as *population-averaged, regularised signals* rather than definitive causal effects. The finding that environmental structure (PCG) can aid perception is consistent with the idea that added texture and edges improve detection/tracking in some lighting conditions, but targeted experiments would be needed to disentangle mechanism from correlation.

5.5 Practical implications for simulation-based ADAS testing

Based on the above, we highlight three actionable guidelines:

- **Include fidelity sweeps, not just clean baselines.** Low-fidelity scenes can systematically *under-expose risk*. Adding illumination geometry (especially low sun) and scene structure can reveal both soft degradations (later/closer activation) and hard failures.
- **Prioritise scenario diversity over global averages.** Effects are *scenario-dependent* in sign and magnitude. Averages can cancel opposing shifts and obscure safety-relevant tails. Coverage across geometry, speeds, occlusion and illumination is more informative than a single pooled effect.
- **Track both margins and failures.** Within-activation margin shifts and outright non-activations are complementary indicators. Both should be first-class metrics in dashboards and CI/CD gates.

5.6 Methodological reflections

Three choices are worth emphasising for readers seeking to reproduce or extend this work:

1. **Baseline alignment via simple paired comparisons:** We summarize cross-simulator agreement with the mean paired difference (95% t -interval), RMSE, the maximum absolute difference, and symmetric percentage differences, and we visualize agreement using identity-line scatter plots and difference-vs-average plots. This keeps the check simple and interpretable.
2. **Within-scenario deltas:** Modelling $\Delta y_{is} = y_{is} - y_s^{(\text{base})}$ enforces a fixed-effects logic that increases comparability across heterogeneous scenarios and mitigates confounding from scenario-level baselines.
3. **Inference under dependence and rarity:** Scenario-level cluster bootstraps acknowledge within-scenario correlation, and ridge penalties guard against overfitting with correlated binaries and few events. Intervals are interpreted cautiously given $K = 16$ clusters and regularisation bias.

5.7 Threats to validity and limitations

We note the following constraints:

- **Scope of stack and sensing.** Results reflect one industry-grade, camera-only perception stack. Transferability to other architectures (e.g., radar/LiDAR fusion) or viewpoints is untested.
- **Rendering space.** We varied shadows, sky, PCG, and sun elevation (with fixed directions excluded from modelling), but did not study auto-exposure, HDR/tone mapping, motion blur, noise, lens flares, adverse weather, or night. All of which are plausible drivers of perception shifts.
- **Selection/conditioning.** Continuous-outcome models are conditioned on activation. If the same factors influence activation, conditioning can induce selection (collider) bias. We therefore interpret within-activation effects as descriptive, not causal.
- **Sparse failures.** With 15 failures total, the failure model is low-EPV. Ridge shrinkage and class weighting help but also bias ORs toward 1; bootstrap CIs reflect resampling uncertainty but do not correct regularisation bias.
- **Small number of clusters.** The cluster bootstrap uses $K = 16$ scenarios. Finite-cluster properties can produce under/over-coverage; this is why we consistently describe intervals as *cautious*.
- **Dynamics abstraction.** `esmini` provides deterministic, idealised actuation. Real vehicle dynamics (tyre friction curves, actuator latencies) could change how perception timing maps to collision risk.

Despite these limitations, two findings are robust across analyses: (i) fidelity changes activation margins in a scenario-dependent manner, and (ii) higher fidelity can expose non-activations that low-fidelity scenes miss.

5.8 Future work

The results suggest several follow-ons:

- **Broaden scenarios and sensors.** Add crossing/merging traffic, urban occlusions, side/rear cameras and sensor fusion to test external validity.
- **Extend fidelity factors.** Night, rain/fog/snow, wet/glossy surfaces, auto-exposure/HDR, motion blur and noise; richer built environments.
- **Model interactions.** Explore interactions (e.g., elevation \times PCG) and non-linearities once sample size allows; consider mixed-effects or cluster-robust models as K grows.
- **Unify margins and failures.** A two-part (hurdle/selection) strategy could jointly model activation probability and conditional margins, clarifying how factors shift both the event and its timing.
- **Track validation.** Targeted track tests under low sun and structured backgrounds to calibrate the predictive value of high-fidelity simulation for AEB.
- **Integrate into continuous integration.** Automate fidelity sweeps and failure tracing with dashboards that surface both margin erosion and non-activations as regression gates.

In summary, increased visual fidelity does not produce a uniform shift in AEB behaviour. Instead, it induces *context-dependent* changes and, in a meaningful fraction of cases, reveals hidden failure modes. Establishing strong cross-simulator baseline agreement via simple matched-pairs comparisons, modelling within-scenario deltas with cluster-aware uncertainty, and explicitly separating margin shifts from activation failures together provide a principled template for simulation-based ADAS validation.

Bibliography

- [1] *Global Status Report on Road Safety 2023*, en, 1st ed. Geneva: World Health Organization, 2023, ISBN: 978-92-4-008651-7.
- [2] J. Nidamanuri, C. Nibhanupudi, R. Assfalg, and H. Venkataraman, “A progressive review: Emerging technologies for adas driven solutions,” *IEEE Transactions on Intelligent Vehicles*, vol. 7, no. 2, pp. 326–341, 2022. DOI: 10.1109/TIV.2021.3122898.
- [3] M. Ellims, “Brake systems: A mind of their own,” *Digital Evidence & Elec. Signature L. Rev.*, vol. 18, p. 27, 2021.
- [4] *New Vehicle General Safety Regulation*, sv, Text. Accessed: Apr. 18, 2025. [Online]. Available: https://ec.europa.eu/commission/presscorner/detail/en/ip_22_4312.
- [5] Unity Technologies, *Universal Render Pipeline Overview*, <https://docs.unity3d.com/Packages/com.unity.render-pipelines.universal@16.0/manual/index.html>, Accessed: 2025-04-23.
- [6] D. Liu, J. Yu, N. D. Macchiarella, and D. A. Vincenzi, “Simulation fidelity,” in *Human factors in simulation and training*, CRC Press, 2008, pp. 91–108.
- [7] ASAM e.V., *ASAM OpenSCENARIO XML Standard*, <https://www.asam.net/standards/detail/openscenario-xml/>, Accessed: 2025-04-22.
- [8] ASAM e.V., *ASAM OpenDRIVE Standard*, <https://www.asam.net/standards/detail/opendrive/>, Accessed: 2025-04-22.
- [9] ASAM e.V., *ASAM OSI Standard*, <https://www.asam.net/standards/detail/osi/>, Accessed: 2025-04-22.
- [10] M. Laukvik and contributors, *esmini — Essential mini openscenario player*, <https://github.com/esmini/esmini>, Accessed: 2025-04-22.
- [11] X. Yang et al., “Drivearena: A closed-loop generative simulation platform for autonomous driving,” *arXiv preprint arXiv:2408.00415*, 2024.
- [12] Euro NCAP, *Euro NCAP AEB C2C Test Protocol - v4.3.1*, <https://www.euroncap.com/media/80155/euro-ncap-aeb-c2c-test-protocol-v431.pdf>, Accessed: 2025-06-14.
- [13] International Organization for Standardization, *Road vehicles – Safety of the intended functionality (SOTIF)*, <https://www.iso.org/standard/77490.html>, ISO 21448:2022, 2022.
- [14] Euro NCAP, *Vision 2030: A Safer Future for Mobility*, <https://cdn.euroncap.com/media/74468/euro-ncap-roadmap-vision-2030.pdf>, Euro NCAP roadmap, published 9November2022, Nov. 2022.

Bibliography

- [15] T. Wang, X. Zhu, J. Pang, and D. Lin, “Fcov3d: Fully convolutional one-stage monocular 3d object detection,” in *Proceedings of the IEEE/CVF international conference on computer vision*, 2021, pp. 913–922.
- [16] Z. Tian, C. Shen, H. Chen, and T. He, “Fcov: Fully convolutional one-stage object detection,” in *Proceedings of the IEEE/CVF international conference on computer vision*, 2019, pp. 9627–9636.
- [17] Unity Technologies, *Introduction to Lightmaps and Baking*, <https://docs.unity3d.com/Manual/Lightmappers.html>, Accessed: 2025-04-23.
- [18] Unity Technologies, *Optimize Your Mobile Game Performance: Expert Tips on Graphics and Assets*, <https://unity.com/blog/games/optimize-your-mobile-game-performance-expert-tips-on-graphics-and-assets>, Accessed: 2025-04-23.
- [19] Epic Games, *Unreal Engine 5.0 Release Notes*, https://dev.epicgames.com/documentation/en-us/unreal-engine/unreal-engine-5.0-release-notes?application_version=5.0, Accessed: 2025-04-23.
- [20] Epic Games, *Path Tracer in Unreal Engine*, <https://dev.epicgames.com/documentation/en-us/unreal-engine/path-tracer-in-unreal-engine/>, Accessed: 2025-04-23.
- [21] Epic Games, *Nanite Virtualized Geometry in Unreal Engine*, <https://dev.epicgames.com/documentation/en-us/unreal-engine/nanite-virtualized-geometry-in-unreal-engine/>, Accessed: 2025-04-23.
- [22] Epic Games, *Lumen Global Illumination and Reflections in Unreal Engine*, <https://dev.epicgames.com/documentation/en-us/unreal-engine/lumen-global-illumination-and-reflections-in-unreal-engine>, Accessed: 2025-04-23.
- [23] D. Hendrycks and T. Dietterich, “Benchmarking neural network robustness to common corruptions and perturbations,” *arXiv preprint arXiv:1903.12261*, 2019.
- [24] R. Geirhos, P. Rubisch, C. Michaelis, M. Bethge, F. A. Wichmann, and W. Brendel, “Imagenet-trained cnns are biased towards texture; increasing shape bias improves accuracy and robustness,” in *International conference on learning representations*, 2018.
- [25] Canonical, *Pipe - overview of pipes and FIFOs*, <https://manpages.ubuntu.com/manpages/focal/man7/pipe.7.html>, Accessed: 2025-05-18.
- [26] Oracle Corporation, *Overview of sockets*, Oracle Solaris 11.1 Programming Interfaces Guide, 2012. [Online]. Available: https://docs.oracle.com/cd/E26502_01/html/E35299/sockets-42163.html.
- [27] Euro NCAP, *Euro NCAP AEB LSS VRU Test Protocol - v4.5.1*, <https://www.euroncap.com/media/80156/euro-ncap-aeb-lss-vru-test-protocol-v451.pdf>, Accessed: 2025-06-14.
- [28] J. M. Wooldridge, *Econometric analysis of cross section and panel data*. MIT press, 2010.
- [29] A. E. Hoerl and R. W. Kennard, “Ridge regression: Biased estimation for nonorthogonal problems,” *Technometrics*, vol. 12, no. 1, pp. 55–67, 1970.
- [30] R. J. Tibshirani and B. Efron, “An introduction to the bootstrap,” *Monographs on statistics and applied probability*, vol. 57, no. 1, pp. 1–436, 1993.

- [31] A. C. Cameron and D. L. Miller, “A practitioners guide to cluster-robust inference,” *Journal of human resources*, vol. 50, no. 2, pp. 317–372, 2015.
- [32] E. B. Wilson, “Probable inference, the law of succession, and statistical inference,” *Journal of the American Statistical Association*, vol. 22, no. 158, pp. 209–212, 1927.
- [33] S. L. Cessie and J. V. Houwelingen, “Ridge estimators in logistic regression,” *Journal of the Royal Statistical Society Series C: Applied Statistics*, vol. 41, no. 1, pp. 191–201, 1992.
- [34] P. Peduzzi, J. Concato, E. Kemper, T. R. Holford, and A. R. Feinstein, “A simulation study of the number of events per variable in logistic regression analysis,” *Journal of clinical epidemiology*, vol. 49, no. 12, pp. 1373–1379, 1996.
- [35] F. Pedregosa et al., “Scikit-learn: Machine learning in python,” *the Journal of machine Learning research*, vol. 12, pp. 2825–2830, 2011.

Bibliography

A

Appendix 1

Per-Scenario AEB Tables

The following tables present raw AEB metric data per variant for each scenario.

A. Appendix 1

Table A.1: AEB metrics for scenario: Car to Car front turn across path (ccf-tap_speed_20_45)

source	aeb_activated	Shadow	PCG	Direction	Elevation	Sky	t_{AEB} [ms]	d_{AEB} [m]	TTC _{AEB} [s]
Unity (Baseline)	True	False	False		90	False	12475	21.992603	0.920000
UE5 (Baseline)	True	False	False		90	False	12475	22.014822	0.920000
UE5	True	False	False		90	True	12350	24.225832	1.040000
UE5	True	False	True		90	False	12550	20.780243	0.860000
UE5	True	False	True		90	True	12550	20.778925	0.840000
UE5	True	True	False		90	False	12475	21.994530	0.920000
UE5	True	True	False		90	True	12475	22.034081	0.920000
UE5	True	True	False	North	10	False	12475	21.979010	0.920000
UE5	True	True	False	North	10	True	12475	21.988857	0.920000
UE5	True	True	False	North	45	False	12475	22.005295	0.920000
UE5	True	True	False	North	45	True	12475	22.046341	0.920000
UE5	True	True	False	East	10	False	12550	20.656324	0.840000
UE5	True	True	False	East	10	True	12550	20.695677	0.840000
UE5	True	True	False	East	45	False	12500	21.573200	0.900000
UE5	True	True	False	East	45	True	12475	22.026516	0.920000
UE5	True	True	False	South	10	False	12550	20.652475	0.840000
UE5	True	True	False	South	10	True	12550	21.058401	0.860000
UE5	True	True	False	South	45	False	12300	24.965027	1.080000
UE5	True	True	False	South	45	True	12350	24.215178	1.040000
UE5	True	True	False	West	10	False	12550	20.641279	0.840000
UE5	True	True	False	West	10	True	12675	18.510876	0.800000
UE5	True	True	False	West	45	False	12525	21.121502	0.860000
UE5	True	True	False	West	45	True	12500	21.600464	0.900000
UE5	True	True	True		90	False	12550	20.698038	0.840000
UE5	True	True	True		90	True	12550	20.685238	0.840000
UE5	True	True	True	North	10	False	12475	22.002485	0.900000
UE5	True	True	True	North	10	True	12325	24.928787	1.060000
UE5	True	True	True	North	45	False	12525	21.086981	0.860000
UE5	True	True	True	North	45	True	12325	24.563889	1.060000
UE5	True	True	True	East	10	False	12325	24.539227	1.060000
UE5	True	True	True	East	10	True	12475	22.005579	0.920000
UE5	True	True	True	East	45	False	12550	20.696495	0.840000
UE5	True	True	True	East	45	True	12475	22.036991	0.920000
UE5	True	True	True	South	10	False	12525	21.048801	0.860000
UE5	True	True	True	South	10	True	12525	21.081856	0.860000
UE5	True	True	True	South	45	False	12475	22.035252	0.920000
UE5	True	True	True	South	45	True	12525	21.104225	0.860000
UE5	True	True	True	West	10	False	12475	21.976866	0.920000
UE5	True	True	True	West	10	True	12525	21.081703	0.860000
UE5	True	True	True	West	45	False	12550	20.663897	0.840000
UE5	True	True	True	West	45	True	12550	20.681263	0.840000

Table A.2: AEB metrics for scenario: Car to Car front turn across path (ccf-tap_speed_20_60)

source	aeb_activated	Shadow	PCG	Direction	Elevation	Sky	t_{AEB} [ms]	d_{AEB} [m]	TTC _{AEB} [s]
Unity (Baseline)	True	False	False		90	False	12700	20.056802	0.700000
UE5 (Baseline)	True	False	False		90	False	12675	21.161491	0.720000
UE5	True	False	False		90	True	12525	24.831383	0.880000
UE5	True	False	True		90	False	12575	23.737257	0.820000
UE5	True	False	True		90	True	12575	23.772440	0.820000
UE5	True	True	False		90	False	12525	24.283733	0.840000
UE5	True	True	False		90	True	12525	24.307631	0.840000
UE5	True	True	False	North	10	False	12550	24.296915	0.860000
UE5	True	True	False	North	10	True	12675	21.126619	0.720000
UE5	True	True	False	North	45	False	12500	24.939432	0.880000
UE5	True	True	False	North	45	True	12525	24.431171	0.860000
UE5	True	True	False	East	10	False	12675	21.117466	0.740000
UE5	True	True	False	East	10	True	12675	21.521057	0.720000
UE5	True	True	False	East	45	False	12675	21.118774	0.700000
UE5	True	True	False	East	45	True	12675	21.262764	0.720000
UE5	True	True	False	South	10	False	12675	21.528154	0.760000
UE5	True	True	False	South	10	True	12675	21.332275	0.720000
UE5	True	True	False	South	45	False	12525	24.261126	0.860000
UE5	True	True	False	South	45	True	12525	24.801699	0.880000
UE5	True	True	False	West	10	False	12725	20.056803	0.700000
UE5	True	True	False	West	10	True	12700	20.608791	0.700000
UE5	True	True	False	West	45	False	12675	21.145290	0.720000
UE5	True	True	False	West	45	True	12675	21.125105	0.700000
UE5	True	True	True		90	False	12475	25.391768	0.900000
UE5	True	True	True		90	True	12525	24.289616	0.840000
UE5	True	True	True	North	10	False	12475	25.380968	0.900000
UE5	True	True	True	North	10	True	12475	25.968382	0.920000
UE5	True	True	True	North	45	False	12675	21.123457	0.740000
UE5	True	True	True	North	45	True	12475	25.384218	0.900000
UE5	True	True	True	East	10	False	12275	29.527004	1.100000
UE5	True	True	True	East	10	True	12525	24.877047	0.880000
UE5	True	True	True	East	45	False	12675	21.204811	0.720000
UE5	True	True	True	East	45	True	12675	21.148750	0.720000
UE5	True	True	True	South	10	False	12675	21.145466	0.720000
UE5	True	True	True	South	10	True	12675	21.277018	0.720000
UE5	True	True	True	South	45	False	12525	24.289600	0.840000
UE5	True	True	True	South	45	True	12525	24.325066	0.840000
UE5	True	True	True	West	10	False	12550	24.314730	0.860000
UE5	True	True	True	West	10	True	12575	23.727911	0.820000
UE5	True	True	True	West	45	False	12675	21.147051	0.720000
UE5	True	True	True	West	45	True	12550	24.320488	0.860000

A. Appendix 1

Table A.3: AEB metrics for scenario: Car to Car Rear braking (ccrb_decel_6)

source	aeb_activated	Shadow	PCG	Direction	Elevation	Sky	t_{AEB} [ms]	d_{AEB} [m]	TTC _{AEB} [s]
Unity (Baseline)	True	False	False		90	False	8425	24.719154	1.360000
UE5 (Baseline)	True	False	False		90	False	8425	24.692036	1.360000
UE5	True	False	False		90	True	8425	24.673859	1.360000
UE5	True	False	True		90	False	8425	24.699368	1.360000
UE5	True	False	True		90	True	8425	24.626497	1.360000
UE5	True	True	False		90	False	8425	24.732346	1.360000
UE5	True	True	False		90	True	8425	24.642298	1.360000
UE5	True	True	False	North	10	False	8425	24.625401	1.360000
UE5	True	True	False	North	10	True	8425	24.749805	1.360000
UE5	True	True	False	North	45	False	8450	24.531530	1.360000
UE5	True	True	False	North	45	True	8425	24.703564	1.360000
UE5	True	True	False	East	10	False	8425	24.646503	1.360000
UE5	True	True	False	East	10	True	8425	24.721703	1.360000
UE5	True	True	False	East	45	False	8425	24.803776	1.380000
UE5	True	True	False	East	45	True	8425	24.669611	1.360000
UE5	True	True	False	South	10	False	8425	24.735056	1.360000
UE5	True	True	False	South	10	True	8425	24.924778	1.360000
UE5	True	True	False	South	45	False	8425	24.791824	1.380000
UE5	True	True	False	South	45	True	8425	24.732981	1.360000
UE5	True	True	False	West	10	False	8425	24.640709	1.360000
UE5	True	True	False	West	10	True	8425	24.812706	1.360000
UE5	True	True	False	West	45	False	8425	24.660370	1.360000
UE5	True	True	False	West	45	True	8425	24.718948	1.360000
UE5	True	True	True		90	False	8425	24.683270	1.360000
UE5	True	True	True		90	True	8425	24.825329	1.380000
UE5	True	True	True	North	10	False	8425	24.725784	1.360000
UE5	True	True	True	North	10	True	8425	24.659800	1.360000
UE5	True	True	True	North	45	False	8425	24.757139	1.360000
UE5	True	True	True	North	45	True	8425	24.642017	1.360000
UE5	True	True	True	East	10	False	8425	24.777044	1.380000
UE5	True	True	True	East	10	True	8425	24.715883	1.360000
UE5	True	True	True	East	45	False	8425	24.733128	1.360000
UE5	True	True	True	East	45	True	8425	24.705868	1.360000
UE5	True	True	True	South	10	False	8425	24.810894	1.380000
UE5	True	True	True	South	10	True	8425	24.791506	1.380000
UE5	True	True	True	South	45	False	8425	24.792330	1.380000
UE5	True	True	True	South	45	True	8425	24.787411	1.380000
UE5	True	True	True	West	10	False	8425	24.718813	1.360000
UE5	True	True	True	West	10	True	8425	24.782213	1.380000
UE5	True	True	True	West	45	False	8425	24.737034	1.360000
UE5	True	True	True	West	45	True	8425	24.718138	1.360000

Table A.4: AEB metrics for scenario: Car to Car Rear braking (ccrb_decel_2)

source	aeb_activated	Shadow	PCG	Direction	Elevation	Sky	t_{AEB} [ms]	d_{AEB} [m]	TTC _{AEB} [s]
Unity (Baseline)	True	False	False		90	False	10950	17.953394	1.160000
UE5 (Baseline)	True	False	False		90	False	10950	18.066757	1.160000
UE5	True	False	False		90	True	10975	17.867014	1.140000
UE5	True	False	True		90	False	10975	17.882547	1.140000
UE5	True	False	True		90	True	10975	17.908859	1.140000
UE5	True	True	False		90	False	10975	17.807655	1.140000
UE5	True	True	False		90	True	10975	17.851891	1.140000
UE5	True	True	False	North	10	False	10975	17.847755	1.140000
UE5	True	True	False	North	10	True	10975	17.813305	1.140000
UE5	True	True	False	North	45	False	10975	17.875277	1.140000
UE5	True	True	False	North	45	True	10975	17.845407	1.140000
UE5	True	True	False	East	10	False	10975	17.842951	1.140000
UE5	True	True	False	East	10	True	10975	17.881237	1.140000
UE5	True	True	False	East	45	False	10975	17.889086	1.140000
UE5	True	True	False	East	45	True	10975	17.799719	1.140000
UE5	True	True	False	South	10	False	10975	17.863354	1.140000
UE5	True	True	False	South	10	True	10950	18.229933	1.160000
UE5	True	True	False	South	45	False	10950	18.096069	1.160000
UE5	True	True	False	South	45	True	10975	17.842146	1.140000
UE5	True	True	False	West	10	False	10975	17.774826	1.140000
UE5	True	True	False	West	10	True	10975	17.916967	1.140000
UE5	True	True	False	West	45	False	10975	17.877695	1.140000
UE5	True	True	False	West	45	True	10975	17.851303	1.140000
UE5	True	True	True		90	False	10975	17.867617	1.140000
UE5	True	True	True		90	True	10975	17.832115	1.140000
UE5	True	True	True	North	10	False	10950	17.970354	1.160000
UE5	True	True	True	North	10	True	10975	17.865471	1.140000
UE5	True	True	True	North	45	False	10950	18.083931	1.160000
UE5	True	True	True	North	45	True	10975	17.838030	1.140000
UE5	True	True	True	East	10	False	10975	17.856756	1.140000
UE5	True	True	True	East	10	True	10975	17.856266	1.140000
UE5	True	True	True	East	45	False	10975	17.863388	1.140000
UE5	True	True	True	East	45	True	10950	18.079185	1.160000
UE5	True	True	True	South	10	False	10975	17.862679	1.140000
UE5	False	True	True	South	10	True			
UE5	True	True	True	South	45	False	10975	17.869759	1.140000
UE5	True	True	True	South	45	True	10950	18.054417	1.160000
UE5	True	True	True	West	10	False	10975	17.920374	1.140000
UE5	True	True	True	West	10	True	10975	17.902483	1.140000
UE5	True	True	True	West	45	False	10975	17.865770	1.140000
UE5	True	True	True	West	45	True	10975	17.827946	1.140000

A. Appendix 1

Table A.5: AEB metrics for scenario: Car to Car Rear moving (ccrm_speed_50)

source	aeb_activated	Shadow	PCG	Direction	Elevation	Sky	t_{AEB} [ms]	d_{AEB} [m]	TTC _{AEB} [s]
Unity (Baseline)	True	False	False		90	False	3600	13.957398	0.980000
UE5 (Baseline)	True	False	False		90	False	3600	13.959739	0.960000
UE5	True	False	False		90	True	3575	14.300638	1
UE5	True	False	True		90	False	3575	14.178730	1
UE5	True	False	True		90	True	3575	14.180910	1
UE5	True	True	False		90	False	3575	14.198496	1
UE5	True	True	False		90	True	3575	14.215182	0.980000
UE5	True	True	False	North	10	False	3600	13.987144	0.980000
UE5	False	True	False	North	10	True			
UE5	True	True	False	North	45	False	3600	14.037857	0.980000
UE5	False	True	False	North	45	True			
UE5	True	True	False	East	10	False	3575	14.213135	1
UE5	True	True	False	East	10	True	3600	14.147773	1
UE5	True	True	False	East	45	False	3600	14.149997	1
UE5	True	True	False	East	45	True	3600	14.152203	1
UE5	True	True	False	South	10	False	3600	14.037913	0.980000
UE5	True	True	False	South	10	True	3600	14.078103	0.960000
UE5	True	True	False	South	45	False	3600	13.942674	0.960000
UE5	True	True	False	South	45	True	3600	14.159604	1
UE5	True	True	False	West	10	False	3600	13.973252	0.980000
UE5	True	True	False	West	10	True	3600	14.039132	0.980000
UE5	True	True	False	West	45	False	3600	14.122407	1
UE5	True	True	False	West	45	True	3600	14.169868	1
UE5	True	True	True		90	False	3575	14.184154	1
UE5	True	True	True		90	True	3550	14.346720	1.020000
UE5	True	True	True	North	10	False	3600	14.014119	0.980000
UE5	True	True	True	North	10	True	3600	14.003082	0.980000
UE5	True	True	True	North	45	False	3600	14.040095	0.980000
UE5	True	True	True	North	45	True	3600	14.060188	0.980000
UE5	True	True	True	East	10	False	3600	13.986871	0.980000
UE5	True	True	True	East	10	True	3600	14.035812	0.980000
UE5	True	True	True	East	45	False	3600	14.175366	1
UE5	True	True	True	East	45	True	3600	14.051320	0.980000
UE5	True	True	True	South	10	False	3600	14.058595	0.980000
UE5	True	True	True	South	10	True	3575	14.206508	1
UE5	True	True	True	South	45	False	3575	14.215167	1
UE5	True	True	True	South	45	True	3600	14.121293	1
UE5	True	True	True	West	10	False	3600	14.057456	0.980000
UE5	True	True	True	West	10	True	3600	14.160439	1
UE5	True	True	True	West	45	False	3600	14.136890	1
UE5	True	True	True	West	45	True	3600	14.098336	1

Table A.6: AEB metrics for scenario: Car to Car Rear moving (ccrm_speed_80)

source	aeb_activated	Shadow	PCG	Direction	Elevation	Sky	t_{AEB} [ms]	d_{AEB} [m]	TTC _{AEB} [s]
Unity (Baseline)	True	False	False		90	False	3425	28.528824	1.380000
UE5 (Baseline)	True	False	False		90	False	3400	29.014679	1.400000
UE5	True	False	False		90	True	3375	29.400280	1.420000
UE5	True	False	True		90	False	3400	29.026175	1.400000
UE5	True	False	True		90	True	3425	28.484865	1.380000
UE5	True	True	False		90	False	3400	28.940065	1.400000
UE5	True	True	False		90	True	3375	29.363411	1.420000
UE5	True	True	False	North	10	False	3400	28.667345	1.380000
UE5	True	True	False	North	10	True	3425	28.551468	1.360000
UE5	True	True	False	North	45	False	3425	28.534414	1.380000
UE5	True	True	False	North	45	True	3400	28.867418	1.400000
UE5	True	True	False	East	10	False	3400	28.794138	1.380000
UE5	True	True	False	East	10	True	3400	28.880877	1.400000
UE5	True	True	False	East	45	False	3400	28.845625	1.400000
UE5	True	True	False	East	45	True	3400	28.890837	1.400000
UE5	True	True	False	South	10	False	3450	28.198927	1.360000
UE5	True	True	False	South	10	True	3350	29.967615	1.440000
UE5	True	True	False	South	45	False	3425	28.514536	1.380000
UE5	True	True	False	South	45	True	3425	28.566452	1.380000
UE5	True	True	False	West	10	False	3425	28.466536	1.380000
UE5	True	True	False	West	10	True	3425	28.713867	1.380000
UE5	True	True	False	West	45	False	3425	28.463831	1.380000
UE5	True	True	False	West	45	True	3400	28.865051	1.400000
UE5	True	True	True		90	False	3400	28.932596	1.400000
UE5	True	True	True		90	True	3400	28.913225	1.400000
UE5	True	True	True	North	10	False	3425	28.556427	1.380000
UE5	True	True	True	North	10	True	3425	28.469187	1.380000
UE5	True	True	True	North	45	False	3400	28.859922	1.400000
UE5	True	True	True	North	45	True	3400	28.807318	1.400000
UE5	True	True	True	East	10	False	3450	28.049444	1.360000
UE5	True	True	True	East	10	True	3425	28.416534	1.360000
UE5	True	True	True	East	45	False	3425	28.632727	1.380000
UE5	True	True	True	East	45	True	3425	28.590738	1.380000
UE5	True	True	True	South	10	False	3425	28.476370	1.380000
UE5	True	True	True	South	10	True	3425	28.493017	1.380000
UE5	True	True	True	South	45	False	3425	28.582336	1.380000
UE5	True	True	True	South	45	True	3425	28.494467	1.380000
UE5	True	True	True	West	10	False	3425	28.419558	1.380000
UE5	True	True	True	West	10	True	3425	28.414314	1.360000
UE5	True	True	True	West	45	False	3425	28.393076	1.360000
UE5	True	True	True	West	45	True	3425	28.493032	1.380000

A. Appendix 1

Table A.7: AEB metrics for scenario: Car to Car Rear stationary (ccrs_speed_50)

source	aeb_activated	Shadow	PCG	Direction	Elevation	Sky	t_{AEB} [ms]	d_{AEB} [m]	TTC _{AEB} [s]
Unity (Baseline)	True	False	False		90	False	13500	23.266449	1.260000
UE5 (Baseline)	True	False	False		90	False	13575	23.459267	1.280000
UE5	True	False	False		90	True	13475	23.651377	1.280000
UE5	True	False	True		90	False	13550	23.777697	1.300000
UE5	True	False	True		90	True	13475	23.548458	1.280000
UE5	True	True	False		90	False	13575	23.565609	1.280000
UE5	True	True	False		90	True	13475	23.666147	1.300000
UE5	True	True	False	North	10	False	13400	23.957798	1.320000
UE5	True	True	False	North	10	True	13675	23.614258	1.280000
UE5	True	True	False	North	45	False	13525	23.664560	1.280000
UE5	True	True	False	North	45	True	13450	23.886814	1.300000
UE5	True	True	False	East	10	False	13475	23.743219	1.300000
UE5	True	True	False	East	10	True	13475	23.589680	1.280000
UE5	True	True	False	East	45	False	13475	23.672819	1.300000
UE5	True	True	False	East	45	True	13575	23.522501	1.280000
UE5	True	True	False	South	10	False	13475	23.678093	1.280000
UE5	True	True	False	South	10	True	13700	23.312923	1.240000
UE5	True	True	False	South	45	False	13550	23.760593	1.300000
UE5	True	True	False	South	45	True	13550	23.816288	1.300000
UE5	True	True	False	West	10	False	13475	23.675817	1.280000
UE5	True	True	False	West	10	True	13450	24.161118	1.320000
UE5	True	True	False	West	45	False	13575	23.426079	1.280000
UE5	True	True	False	West	45	True	13575	23.506104	1.280000
UE5	True	True	True		90	False	13450	23.911760	1.300000
UE5	True	True	True		90	True	13550	23.737492	1.300000
UE5	True	True	True	North	10	False	13475	23.626026	1.280000
UE5	True	True	True	North	10	True	13575	23.436213	1.280000
UE5	True	True	True	North	45	False	13450	23.875713	1.300000
UE5	True	True	True	North	45	True	13450	23.851122	1.300000
UE5	True	True	True	East	10	False	13575	23.638645	1.280000
UE5	True	True	True	East	10	True	13450	24.015095	1.320000
UE5	True	True	True	East	45	False	13450	23.997772	1.320000
UE5	True	True	True	East	45	True	13450	23.889475	1.300000
UE5	True	True	True	South	10	False	13475	23.554743	1.280000
UE5	True	True	True	South	10	True	13500	23.338823	1.260000
UE5	True	True	True	South	45	False	13525	23.679308	1.300000
UE5	True	True	True	South	45	True	13575	23.538130	1.280000
UE5	True	True	True	West	10	False	13450	24.043760	1.320000
UE5	True	True	True	West	10	True	13475	23.858736	1.300000
UE5	True	True	True	West	45	False	13475	23.550318	1.280000
UE5	True	True	True	West	45	True	13475	23.639668	1.280000

Table A.8: AEB metrics for scenario: Car to Car Rear stationary (ccrs_speed_80)

source	aeb_activated	Shadow	PCG	Direction	Elevation	Sky	t_{AEB} [ms]	d_{AEB} [m]	TTC _{AEB} [s]
Unity (Baseline)	True	False	False		90	False	13450	36.470341	1.380000
UE5 (Baseline)	True	False	False		90	False	13425	37.045891	1.420000
UE5	True	False	False		90	True	13425	37.045418	1.420000
UE5	True	False	True		90	False	13400	37.478279	1.440000
UE5	True	False	True		90	True	13425	37.041500	1.420000
UE5	True	True	False		90	False	13425	37.050018	1.420000
UE5	True	True	False		90	True	13425	37.043541	1.420000
UE5	True	True	False	North	10	False	14075	24.878700	0.860000
UE5	True	True	False	North	10	True	14150	23.369761	0.800000
UE5	True	True	False	North	45	False	13425	37.086670	1.420000
UE5	True	True	False	North	45	True	13400	37.680340	1.440000
UE5	True	True	False	East	10	False	13450	36.472614	1.380000
UE5	True	True	False	East	10	True	13450	36.317150	1.380000
UE5	True	True	False	East	45	False	13425	36.993423	1.400000
UE5	True	True	False	East	45	True	13400	37.579510	1.440000
UE5	True	True	False	South	10	False	13425	37.089359	1.420000
UE5	True	True	False	South	10	True	13750	29.658209	1.080000
UE5	True	True	False	South	45	False	13425	37.078281	1.420000
UE5	True	True	False	South	45	True	13425	37.033607	1.420000
UE5	True	True	False	West	10	False	13425	37.007584	1.400000
UE5	True	True	False	West	10	True	13400	37.792343	1.440000
UE5	True	True	False	West	45	False	13400	37.540424	1.440000
UE5	True	True	False	West	45	True	13400	37.564384	1.440000
UE5	True	True	True		90	False	13425	37.020130	1.420000
UE5	True	True	True		90	True	13425	37.049717	1.420000
UE5	True	True	True	North	10	False	14075	23.012762	0.780000
UE5	True	True	True	North	10	True	14150	23.378338	0.800000
UE5	True	True	True	North	45	False	13400	37.579559	1.440000
UE5	True	True	True	North	45	True	13425	37.046478	1.420000
UE5	True	True	True	East	10	False	14150	24.320620	0.840000
UE5	True	True	True	East	10	True	13825	27.737616	1
UE5	True	True	True	East	45	False	13400	37.433487	1.420000
UE5	True	True	True	East	45	True	13425	36.596107	1.400000
UE5	True	True	True	South	10	False	13425	37.071499	1.420000
UE5	True	True	True	South	10	True	13550	32.491314	1.200000
UE5	True	True	True	South	45	False	13425	37.038853	1.420000
UE5	True	True	True	South	45	True	13425	37.030640	1.420000
UE5	True	True	True	West	10	False	13950	25.976574	0.920000
UE5	True	True	True	West	10	True	13475	35.599724	1.340000
UE5	True	True	True	West	45	False	13400	37.351711	1.420000
UE5	True	True	True	West	45	True	13400	37.359467	1.420000

A. Appendix 1

Table A.9: AEB metrics for scenario: Car to Pedestrian Farside Adult (cpfa_speed_50)

source	aeb_activated	Shadow	PCG	Direction	Elevation	Sky	t_{AEB} [ms]	d_{AEB} [m]	TTC _{AEB} [s]
Unity (Baseline)	True	False	False		90	False	7850	20.132771	1.160000
UE5 (Baseline)	True	False	False		90	False	7775	21.170599	1.240000
UE5	True	False	False		90	True	7775	21.170397	1.240000
UE5	True	False	True		90	False	7775	21.181952	1.240000
UE5	True	False	True		90	True	7775	21.183867	1.240000
UE5	True	True	False		90	False	7775	21.170731	1.240000
UE5	True	True	False		90	True	7775	21.170084	1.240000
UE5	True	True	False	North	10	False	7775	21.174850	1.240000
UE5	True	True	False	North	10	True	7775	21.168756	1.240000
UE5	True	True	False	North	45	False	7775	21.167816	1.240000
UE5	True	True	False	North	45	True	7775	21.161400	1.240000
UE5	True	True	False	East	10	False	7825	20.495630	1.180000
UE5	True	True	False	East	10	True	7775	21.160833	1.240000
UE5	True	True	False	East	45	False	7775	21.161856	1.240000
UE5	True	True	False	East	45	True	7775	21.164366	1.240000
UE5	True	True	False	South	10	False	7775	21.164310	1.240000
UE5	True	True	False	South	10	True	7775	21.165997	1.240000
UE5	True	True	False	South	45	False	7775	21.172081	1.240000
UE5	True	True	False	South	45	True	7775	21.172581	1.240000
UE5	True	True	False	West	10	False	7875	19.811607	1.140000
UE5	True	True	False	West	10	True	7775	21.164022	1.240000
UE5	True	True	False	West	45	False	7775	21.165865	1.240000
UE5	True	True	False	West	45	True	7775	21.168169	1.240000
UE5	True	True	True		90	False	7775	21.186045	1.240000
UE5	True	True	True		90	True	7750	21.531912	1.260000
UE5	True	True	True	North	10	False	7825	20.496010	1.180000
UE5	True	True	True	North	10	True	7825	20.482037	1.180000
UE5	True	True	True	North	45	False	7775	21.184998	1.240000
UE5	True	True	True	North	45	True	7775	21.184132	1.240000
UE5	True	True	True	East	10	False	7875	19.809765	1.140000
UE5	True	True	True	East	10	True	7925	19.088921	1.080000
UE5	True	True	True	East	45	False	7775	21.176905	1.240000
UE5	True	True	True	East	45	True	7775	21.176933	1.240000
UE5	True	True	True	South	10	False	7775	21.192623	1.240000
UE5	True	True	True	South	10	True	7775	21.197199	1.240000
UE5	True	True	True	South	45	False	7775	21.188972	1.240000
UE5	True	True	True	South	45	True	7750	21.530403	1.260000
UE5	True	True	True	West	10	False	7875	19.807159	1.140000
UE5	True	True	True	West	10	True	7775	21.208843	1.240000
UE5	True	True	True	West	45	False	7975	18.395506	1.040000
UE5	True	True	True	West	45	True	7800	20.820536	1.220000

Table A.10: AEB metrics for scenario: Car to Pedestrian Farside Adult (cpfa_speed_60)

source	aeb_activated	Shadow	PCG	Direction	Elevation	Sky	t_{AEB} [ms]	d_{AEB} [m]	TTC _{AEB} [s]
Unity (Baseline)	True	False	False		90	False	7850	23.251616	1.160000
UE5 (Baseline)	True	False	False		90	False	7775	24.513674	1.240000
UE5	True	False	False		90	True	7775	24.514751	1.240000
UE5	True	False	True		90	False	7775	24.524948	1.240000
UE5	True	False	True		90	True	7775	24.525517	1.240000
UE5	True	True	False		90	False	7775	24.512854	1.240000
UE5	True	True	False		90	True	7775	24.514141	1.240000
UE5	True	True	False	North	10	False	7775	24.512440	1.240000
UE5	True	True	False	North	10	True	7775	24.501425	1.240000
UE5	True	True	False	North	45	False	7775	24.505507	1.240000
UE5	True	True	False	North	45	True	7775	24.495602	1.220000
UE5	True	True	False	East	10	False	7950	21.604086	1.060000
UE5	True	True	False	East	10	True	7775	24.502693	1.240000
UE5	True	True	False	East	45	False	7775	24.504587	1.240000
UE5	True	True	False	East	45	True	7775	24.508856	1.240000
UE5	True	True	False	South	10	False	7775	24.504879	1.220000
UE5	True	True	False	South	10	True	7775	24.499088	1.220000
UE5	True	True	False	South	45	False	7775	24.512865	1.240000
UE5	True	True	False	South	45	True	7775	24.513147	1.240000
UE5	True	True	False	West	10	False	7975	21.206884	1.040000
UE5	True	True	False	West	10	True	7775	24.503752	1.240000
UE5	True	True	False	West	45	False	7775	24.501045	1.220000
UE5	True	True	False	West	45	True	7775	24.508175	1.240000
UE5	True	True	True		90	False	7775	24.528086	1.240000
UE5	True	True	True		90	True	7775	24.528774	1.240000
UE5	True	True	True	North	10	False	7775	24.515644	1.240000
UE5	True	True	True	North	10	True	7825	23.674494	1.180000
UE5	True	True	True	North	45	False	7800	24.092155	1.200000
UE5	True	True	True	North	45	True	7800	24.090969	1.200000
UE5	True	True	True	East	10	False	7975	21.198139	1.040000
UE5	True	True	True	East	10	True	8025	20.356506	0.980000
UE5	True	True	True	East	45	False	7775	24.515965	1.240000
UE5	True	True	True	East	45	True	7775	24.521177	1.240000
UE5	True	True	True	South	10	False	7775	24.526501	1.240000
UE5	True	True	True	South	10	True	7775	24.511652	1.240000
UE5	True	True	True	South	45	False	7775	24.525038	1.240000
UE5	True	True	True	South	45	True	7775	24.526005	1.240000
UE5	True	True	True	West	10	False	7925	22.017294	1.080000
UE5	True	True	True	West	10	True	7975	21.214239	1.040000
UE5	True	True	True	West	45	False	7850	23.243866	1.160000
UE5	True	True	True	West	45	True	7825	23.671610	1.180000

A. Appendix 1

Table A.11: AEB metrics for scenario: Car to Pedestrian Longitudinal Adult (cpla_speed_50)

source	aeb_activated	Shadow	PCG	Direction	Elevation	Sky	t_{AEB} [ms]	d_{AEB} [m]	TTC _{AEB} [s]
Unity (Baseline)	True	False	False		90	False	5225	18.670464	1.220000
UE5 (Baseline)	True	False	False		90	False	5225	18.670464	1.220000
UE5	False	False	False		90	True			
UE5	True	False	True		90	False	5225	18.648870	1.220000
UE5	True	False	True		90	True	5200	18.691282	1.220000
UE5	False	True	False		90	False			
UE5	True	True	False		90	True	5175	18.967342	1.240000
UE5	True	True	False	North	10	False	5225	18.650328	1.220000
UE5	False	True	False	North	10	True			
UE5	True	True	False	North	45	False	5175	18.922821	1.240000
UE5	False	True	False	North	45	True			
UE5	True	True	False	East	10	False	5175	18.918383	1.240000
UE5	True	True	False	East	10	True	5175	18.921810	1.240000
UE5	False	True	False	East	45	False			
UE5	True	True	False	East	45	True	5175	18.965017	1.240000
UE5	True	True	False	South	10	False	5175	18.939972	1.240000
UE5	True	True	False	South	10	True	5175	18.893826	1.240000
UE5	False	True	False	South	45	False			
UE5	True	True	False	South	45	True	5200	18.896479	1.240000
UE5	True	True	False	West	10	False	5200	18.908611	1.240000
UE5	True	True	False	West	10	True	5175	18.977615	1.240000
UE5	True	True	False	West	45	False	5200	18.635159	1.220000
UE5	True	True	False	West	45	True	5200	18.787025	1.240000
UE5	False	True	True		90	False			
UE5	False	True	True		90	True			
UE5	True	True	True	North	10	False	5300	18.346264	1.180000
UE5	True	True	True	North	10	True	5175	18.971188	1.240000
UE5	True	True	True	North	45	False	5200	18.698898	1.220000
UE5	True	True	True	North	45	True	5175	18.935560	1.240000
UE5	True	True	True	East	10	False	5275	18.506298	1.200000
UE5	True	True	True	East	10	True	5225	18.670464	1.220000
UE5	True	True	True	East	45	False	5200	18.931341	1.240000
UE5	True	True	True	East	45	True	5200	18.939804	1.240000
UE5	True	True	True	South	10	False	5175	18.913832	1.240000
UE5	True	True	True	South	10	True	5175	18.925900	1.240000
UE5	True	True	True	South	45	False	5175	18.969923	1.240000
UE5	True	True	True	South	45	True	5175	18.939837	1.240000
UE5	True	True	True	West	10	False	5300	17.838709	1.160000
UE5	True	True	True	West	10	True	5175	19.054850	1.240000
UE5	True	True	True	West	45	False	5200	18.799520	1.240000
UE5	True	True	True	West	45	True	5225	18.665379	1.220000

Table A.12: AEB metrics for scenario: Car to Pedestrian Longitudinal Adult (cpla_speed_80)

source	aeb_activated	Shadow	PCG	Direction	Elevation	Sky	t_{AEB} [ms]	d_{AEB} [m]	TTC _{AEB} [s]
Unity (Baseline)	True	False	False		90	False	4850	32.261547	1.360000
UE5 (Baseline)	True	False	False		90	False	4825	32.791924	1.380000
UE5	True	False	False		90	True	4850	32.236458	1.360000
UE5	True	False	True		90	False	4850	32.436893	1.360000
UE5	True	False	True		90	True	4825	32.792137	1.380000
UE5	True	True	False		90	False	4850	32.266579	1.360000
UE5	True	True	False		90	True	4850	32.236504	1.360000
UE5	True	True	False	North	10	False	4825	32.810741	1.380000
UE5	True	True	False	North	10	True	4875	31.880730	1.340000
UE5	True	True	False	North	45	False	4850	32.253445	1.360000
UE5	True	True	False	North	45	True	4875	31.717182	1.320000
UE5	True	True	False	East	10	False	4825	32.679329	1.380000
UE5	True	True	False	East	10	True	4850	32.448093	1.360000
UE5	True	True	False	East	45	False	4825	32.787041	1.380000
UE5	True	True	False	East	45	True	4825	32.788834	1.380000
UE5	True	True	False	South	10	False	4875	31.707197	1.320000
UE5	True	True	False	South	10	True	4850	32.123440	1.360000
UE5	True	True	False	South	45	False	4875	31.889767	1.340000
UE5	True	True	False	South	45	True	4900	31.369726	1.320000
UE5	True	True	False	West	10	False	4775	33.686771	1.420000
UE5	True	True	False	West	10	True	4825	32.794167	1.380000
UE5	True	True	False	West	45	False	4875	31.747435	1.340000
UE5	True	True	False	West	45	True	4850	32.437420	1.360000
UE5	True	True	True		90	False	4825	32.751667	1.380000
UE5	True	True	True		90	True	4850	32.270611	1.360000
UE5	True	True	True	North	10	False	5025	28.488304	1.180000
UE5	True	True	True	North	10	True	4850	32.133858	1.360000
UE5	True	True	True	North	45	False	4850	32.260624	1.360000
UE5	True	True	True	North	45	True	4850	32.255733	1.360000
UE5	True	True	True	East	10	False	4825	33.052925	1.360000
UE5	True	True	True	East	10	True	4825	32.705723	1.380000
UE5	True	True	True	East	45	False	4900	31.796093	1.360000
UE5	True	True	True	East	45	True	4850	32.230152	1.360000
UE5	True	True	True	South	10	False	4875	31.876381	1.340000
UE5	True	True	True	South	10	True	4850	32.121925	1.360000
UE5	True	True	True	South	45	False	4850	32.170673	1.360000
UE5	True	True	True	South	45	True	4875	31.671534	1.320000
UE5	True	True	True	West	10	False	4875	32.226093	1.340000
UE5	True	True	True	West	10	True	4825	32.657642	1.380000
UE5	True	True	True	West	45	False	4875	31.746912	1.340000
UE5	True	True	True	West	45	True	4950	30.833418	1.320000

A. Appendix 1

Table A.13: AEB metrics for scenario: Car to Pedestrian Nearside Adult (cpna_speed_50)

source	aeb_activated	Shadow	PCG	Direction	Elevation	Sky	t_{AEB} [ms]	d_{AEB} [m]	TTC _{AEB} [s]
Unity (Baseline)	True	False	False		90	False	7825	20.433614	1.180000
UE5 (Baseline)	True	False	False		90	False	7825	20.430323	1.180000
UE5	True	False	False		90	True	7825	20.434738	1.180000
UE5	True	False	True		90	False	7825	20.437914	1.180000
UE5	True	False	True		90	True	7825	20.441677	1.180000
UE5	True	True	False		90	False	7825	20.428402	1.180000
UE5	True	True	False		90	True	7825	20.435299	1.180000
UE5	True	True	False	North	10	False	7825	20.417156	1.180000
UE5	True	True	False	North	10	True	7825	20.423988	1.180000
UE5	True	True	False	North	45	False	7825	20.427738	1.180000
UE5	True	True	False	North	45	True	7825	20.421307	1.180000
UE5	True	True	False	East	10	False	7825	20.420332	1.180000
UE5	True	True	False	East	10	True	7825	20.416868	1.180000
UE5	True	True	False	East	45	False	7825	20.422045	1.180000
UE5	True	True	False	East	45	True	7825	20.427790	1.180000
UE5	True	True	False	South	10	False	7825	20.425186	1.180000
UE5	True	True	False	South	10	True	7850	20.029562	1.160000
UE5	True	True	False	South	45	False	7825	20.427444	1.180000
UE5	True	True	False	South	45	True	7825	20.434334	1.180000
UE5	True	True	False	West	10	False	7825	20.399633	1.180000
UE5	True	True	False	West	10	True	7825	20.436758	1.180000
UE5	True	True	False	West	45	False	7825	20.421583	1.180000
UE5	True	True	False	West	45	True	7825	20.428967	1.180000
UE5	True	True	True		90	False	7775	21.142591	1.240000
UE5	True	True	True		90	True	7775	21.145655	1.240000
UE5	True	True	True	North	10	False	7775	21.128147	1.240000
UE5	True	True	True	North	10	True	7825	20.423986	1.180000
UE5	True	True	True	North	45	False	7825	20.439974	1.180000
UE5	True	True	True	North	45	True	7775	21.140913	1.240000
UE5	True	True	True	East	10	False	7775	21.130575	1.240000
UE5	True	True	True	East	10	True	7975	18.388239	1.040000
UE5	True	True	True	East	45	False	7825	20.437714	1.180000
UE5	True	True	True	East	45	True	7825	20.455101	1.180000
UE5	True	True	True	South	10	False	7825	20.434692	1.180000
UE5	True	True	True	South	10	True	7775	21.120731	1.240000
UE5	True	True	True	South	45	False	7775	21.138309	1.240000
UE5	True	True	True	South	45	True	7800	20.780373	1.200000
UE5	True	True	True	West	10	False	7825	20.470520	1.180000
UE5	True	True	True	West	10	True	7975	18.422060	1.040000
UE5	True	True	True	West	45	False	7775	21.139494	1.240000
UE5	True	True	True	West	45	True	7775	21.127869	1.240000

Table A.14: AEB metrics for scenario: Car to Pedestrian Nearside Adult (cpna_speed_60)

source	aeb_activated	Shadow	PCG	Direction	Elevation	Sky	t_{AEB} [ms]	d_{AEB} [m]	TTC _{AEB} [s]
Unity (Baseline)	True	False	False		90	False	7900	22.432718	1.100000
UE5 (Baseline)	True	False	False		90	False	7800	24.143545	1.200000
UE5	True	False	False		90	True	7800	24.149820	1.200000
UE5	True	False	True		90	False	7775	24.598810	1.240000
UE5	True	False	True		90	True	7775	24.606062	1.240000
UE5	True	True	False		90	False	7825	23.731644	1.180000
UE5	True	True	False		90	True	7800	24.149328	1.200000
UE5	True	True	False	North	10	False	7775	24.555496	1.240000
UE5	True	True	False	North	10	True	7775	24.581764	1.240000
UE5	True	True	False	North	45	False	7825	23.734491	1.180000
UE5	True	True	False	North	45	True	7825	23.730953	1.180000
UE5	True	True	False	East	10	False	7725	25.428207	1.280000
UE5	True	True	False	East	10	True	7775	24.587732	1.240000
UE5	True	True	False	East	45	False	7775	24.565908	1.240000
UE5	True	True	False	East	45	True	7800	24.144627	1.200000
UE5	True	True	False	South	10	False	7825	23.719654	1.180000
UE5	True	True	False	South	10	True	7775	24.582682	1.240000
UE5	True	True	False	South	45	False	7800	24.142698	1.200000
UE5	True	True	False	South	45	True	7775	24.579433	1.240000
UE5	True	True	False	West	10	False	8025	20.318312	0.980000
UE5	True	True	False	West	10	True	7775	24.577637	1.240000
UE5	True	True	False	West	45	False	7800	24.142691	1.200000
UE5	True	True	False	West	45	True	7825	23.728725	1.180000
UE5	True	True	True		90	False	7800	24.175282	1.220000
UE5	True	True	True		90	True	7775	24.613287	1.240000
UE5	True	True	True	North	10	False	7775	24.594763	1.240000
UE5	True	True	True	North	10	True	7875	22.918505	1.140000
UE5	True	True	True	North	45	False	7775	24.584764	1.240000
UE5	True	True	True	North	45	True	7875	22.908951	1.140000
UE5	True	True	True	East	10	False	7875	22.952164	1.140000
UE5	True	True	True	East	10	True	8250	16.625271	0.760000
UE5	True	True	True	East	45	False	7775	24.597067	1.240000
UE5	True	True	True	East	45	True	7775	24.600988	1.240000
UE5	True	True	True	South	10	False	7775	24.600492	1.240000
UE5	True	True	True	South	10	True	7775	24.581869	1.240000
UE5	True	True	True	South	45	False	7775	24.595150	1.240000
UE5	True	True	True	South	45	True	7775	24.598782	1.240000
UE5	True	True	True	West	10	False	7775	24.604622	1.240000
UE5	True	True	True	West	10	True	8100	19.071049	0.900000
UE5	True	True	True	West	45	False	7775	24.590113	1.240000
UE5	True	True	True	West	45	True	7775	24.579037	1.240000

A. Appendix 1

Table A.15: AEB metrics for scenario: Car to Pedestrian Nearside Child Obstructed (cpnco_speed_50)

source	aeb_activated	Shadow	PCG	Direction	Elevation	Sky	t_{AEB} [ms]	d_{AEB} [m]	TTC _{AEB} [s]
Unity (Baseline)	True	False	False		90	False	7975	18.414640	1.040000
UE5 (Baseline)	True	False	False		90	False	7900	19.495506	1.100000
UE5	False	False	False		90	True			
UE5	True	False	True		90	False	7875	19.768755	1.140000
UE5	True	False	True		90	True	7975	18.422293	1.040000
UE5	True	True	False		90	False	7975	18.452734	1.040000
UE5	True	True	False		90	True	7875	19.764744	1.120000
UE5	True	True	False	North	10	False	8350	14.008658	0.700000
UE5	True	True	False	North	10	True	8250	14.513721	0.760000
UE5	True	True	False	North	45	False	7975	18.433289	1.040000
UE5	True	True	False	North	45	True	7975	18.402502	1.040000
UE5	True	True	False	East	10	False	8250	14.509875	0.740000
UE5	True	True	False	East	10	True	8000	18.053556	1.020000
UE5	True	True	False	East	45	False	7825	20.431211	1.180000
UE5	True	True	False	East	45	True	7875	19.758642	1.140000
UE5	True	True	False	South	10	False	7900	19.492857	1.100000
UE5	True	True	False	South	10	True	7850	20.045416	1.160000
UE5	True	True	False	South	45	False	7975	18.474640	1.040000
UE5	True	True	False	South	45	True	8225	14.883404	0.780000
UE5	True	True	False	West	10	False	8675	9.551875	0.400000
UE5	True	True	False	West	10	True	8225	14.894769	0.780000
UE5	True	True	False	West	45	False	8050	17.344381	0.960000
UE5	True	True	False	West	45	True	8025	17.696676	0.980000
UE5	True	True	True		90	False	8150	15.877398	0.860000
UE5	True	True	True		90	True	8175	15.539079	0.820000
UE5	True	True	True	North	10	False	8175	15.560305	0.820000
UE5	True	True	True	North	10	True	8375	12.767088	0.620000
UE5	True	True	True	North	45	False	8175	15.546997	0.820000
UE5	True	True	True	North	45	True	8175	15.556678	0.820000
UE5	True	True	True	East	10	False	8225	14.879871	0.780000
UE5	True	True	True	East	10	True	8250	14.546817	0.760000
UE5	True	True	True	East	45	False	8175	15.537661	0.820000
UE5	True	True	True	East	45	True	8100	16.632729	0.900000
UE5	True	True	True	South	10	False	8225	14.885742	0.780000
UE5	True	True	True	South	10	True	8275	14.553331	0.760000
UE5	True	True	True	South	45	False	8100	16.651987	0.900000
UE5	True	True	True	South	45	True	8100	16.635059	0.900000
UE5	True	True	True	West	10	False	8275	15.437057	0.800000
UE5	True	True	True	West	10	True	8425	12.138608	0.580000
UE5	True	True	True	West	45	False	8325	13.485094	0.680000
UE5	True	True	True	West	45	True	8000	18.004488	1

Table A.16: AEB metrics for scenario: Car to Pedestrian Nearside Child Obstructed (cpnco_speed_60)

source	aeb_activated	Shadow	PCG	Direction	Elevation	Sky	t_{AEB} [ms]	d_{AEB} [m]	TTC _{AEB} [s]
Unity (Baseline)	True	False	False		90	False	7975	21.234196	1.020000
UE5 (Baseline)	True	False	False		90	False	8050	19.980902	0.960000
UE5	False	False	False		90	True			
UE5	True	False	True		90	False	7975	21.211634	1.040000
UE5	True	False	True		90	True	7975	21.401428	1.040000
UE5	True	True	False		90	False	8200	17.670412	0.820000
UE5	True	True	False		90	True	8050	20.081051	0.960000
UE5	True	True	False	North	10	False	8050	20.004333	0.960000
UE5	True	True	False	North	10	True	8150	18.375706	0.860000
UE5	True	True	False	North	45	False	8650	11.122294	0.420000
UE5	True	True	False	North	45	True	7900	22.530161	1.100000
UE5	True	True	False	East	10	False	8250	16.705299	0.760000
UE5	True	True	False	East	10	True	8150	18.376335	0.860000
UE5	True	True	False	East	45	False	7975	21.264961	1.040000
UE5	True	True	False	East	45	True	8200	17.635790	0.820000
UE5	True	True	False	South	10	False	8075	19.810110	0.940000
UE5	True	True	False	South	10	True	8150	18.767038	0.880000
UE5	True	True	False	South	45	False	7950	21.744860	1.060000
UE5	True	True	False	South	45	True	7975	21.242659	1.040000
UE5	False	True	False	West	10	False			
UE5	True	True	False	West	10	True	7975	21.195585	1.040000
UE5	False	True	False	West	45	False			
UE5	True	True	False	West	45	True	7975	21.251320	1.040000
UE5	True	True	True		90	False	8050	20.081270	0.960000
UE5	True	True	True		90	True	8075	19.655746	0.940000
UE5	True	True	True	North	10	False	8150	18.395746	0.860000
UE5	True	True	True	North	10	True	8250	16.710253	0.760000
UE5	True	True	True	North	45	False	8275	16.261009	0.740000
UE5	True	True	True	North	45	True	8050	20.016195	0.960000
UE5	True	True	True	East	10	False	8325	15.472323	0.680000
UE5	True	True	True	East	10	True	8425	13.835559	0.600000
UE5	True	True	True	East	45	False	7950	21.661390	1.060000
UE5	True	True	True	East	45	True	8050	20.047468	0.960000
UE5	True	True	True	South	10	False	8275	17.274683	0.780000
UE5	True	True	True	South	10	True	8000	20.875786	1.020000
UE5	True	True	True	South	45	False	8150	18.435328	0.860000
UE5	True	True	True	South	45	True	7875	22.920420	1.140000
UE5	True	True	True	West	10	False	8050	20.157181	0.960000
UE5	True	True	True	West	10	True	8375	14.902132	0.660000
UE5	True	True	True	West	45	False	8075	19.586861	0.940000
UE5	True	True	True	West	45	True	8125	18.726536	0.880000